Second Afternoon Session

OPEN DISCUSSION

Melvin W. First, Moderator
Harvard Air Cleaning Laboratory

FIRST: There were ten brief presentations listed on the advanced program. Only nine of those will be offered. I have been offered another, however, which I will announce at the time it is presented at the very end of the discussion.

The rules of the game for this part of the meeting are to present the paper briefly and then we'll have commentary on it and then pass on to the next one.

The program indicates that the papers will be of brief duration, five or ten minutes. In view of the large number we have been offered, I'm going to ask the speakers if they will please try to stay within the five minute period rather than the ten.

Please present only the most essential information. There will be ample opportunity to present all of the details in the written proceedings.

The first presentation, by A. A. Moghissi, H. L. Kelly and C. R. Phillips, is entitled "A Tritium Air Monitor."

A TRITIUM AIR MONITOR

by

A. A. Moghissi, H. L. Kelley, C. R. Phillips

The monitoring of gaseous radionuclides is of particular interest in the determination of efficiency of air cleaning devices. Although the measurement of gamma-emitting nuclides in air is relatively simple, beta-emitting radionuclides present problems. These problems are particularly severe in cases such as tritium, ^{14}C and ^{85}Kr.

Geiger-Müller and proportional counters cannot be effectively used when air is introduced into the counter. For this reason the only continuous radiation monitoring devices with reasonable sensitivity in use are ionization chambers. Although the development of stable circuitry has made it possible to construct highly sensitive monitors, the lack of energy discrimination places limitation on their use.

Another means of detection of beta-emitting radionuclides involves the application of scintillation. The development of bialkali photomultipliers and better electronic components, such as summing amplifiers and nanosecond coincidence units, has created new possibilities for the construction of this type of monitor.

A tritium monitor based on scintillation has been developed at the Southeastern Radiological Health Laboratory. The electronic equipment is to a great extent identical to the components used in commercially available liquid scintillation counters. A block diagram of the monitor is shown in Figure 1.

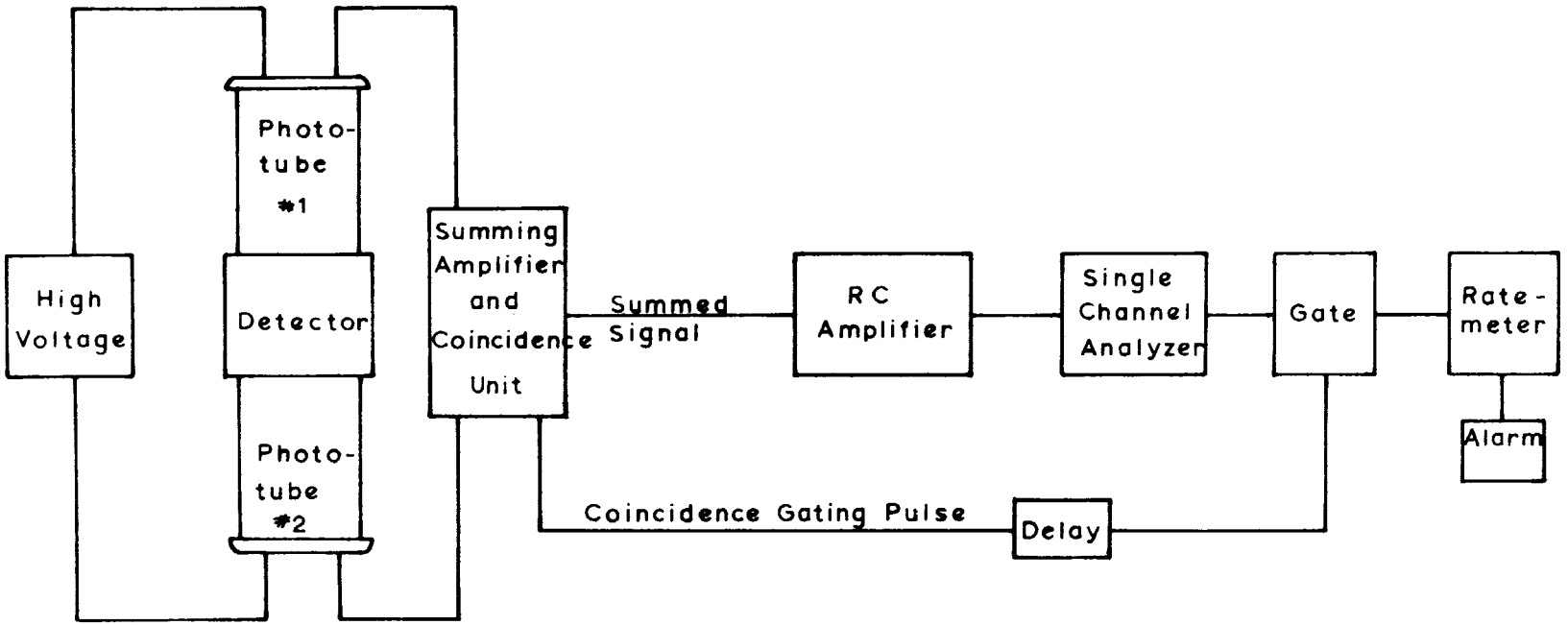

Figure 1. Block diagram of the tritium monitor

The light produced in the detection chamber is registered by two photomultipliers and the resulting pulses are transferred to the coincidence circuit. If the pulses from the two photomultipliers arrive in this unit within 30-50 nanoseconds, the signals are transferred to the summing amplifier where they are added and amplified. A single-channel analyzer is used to select the desired energy range, and the count rate is measured by the ratemeter. Alarm circuitry is added for convenience. Only one high-voltage supply is used for both photomultipliers which requires preselection and matching of the photomultipliers.

Two prototypes of scintillation detection chambers have been developed. The first chamber consists of a cube with 40 parallel plates of plastic phosphor (NE 101 Nuclear Enterprises, Winnepeg 21, Manitoba, Canada) housed in a plexiglass container. Windows for the 2" photomultipliers consist of Teflon sheets 0.3 mm thick. This chamber had essentially the same sensitivity as the second detection chamber and was considerably more sensitive than presently available tritium monitors. It had, however, several disadvantages. Air flow occasionally produced static electricity and the memory effect for tritiated water proved to be severe, making an accurate evaluation of the monitor difficult. The gamma sensitivity of this detector was high and the price of $5 for each plate of plastic phosphor made the detector relatively expensive.

A schematic diagram of the second detection chamber is shown in Figure 2. It consists of 3 mm diameter plexiglass rods coated with anthracene and arranged within a cylindrical chamber. The outer container is 56 mm ID plexiglass pipe 45 mm long with a useful volume of 80 ml. The rods

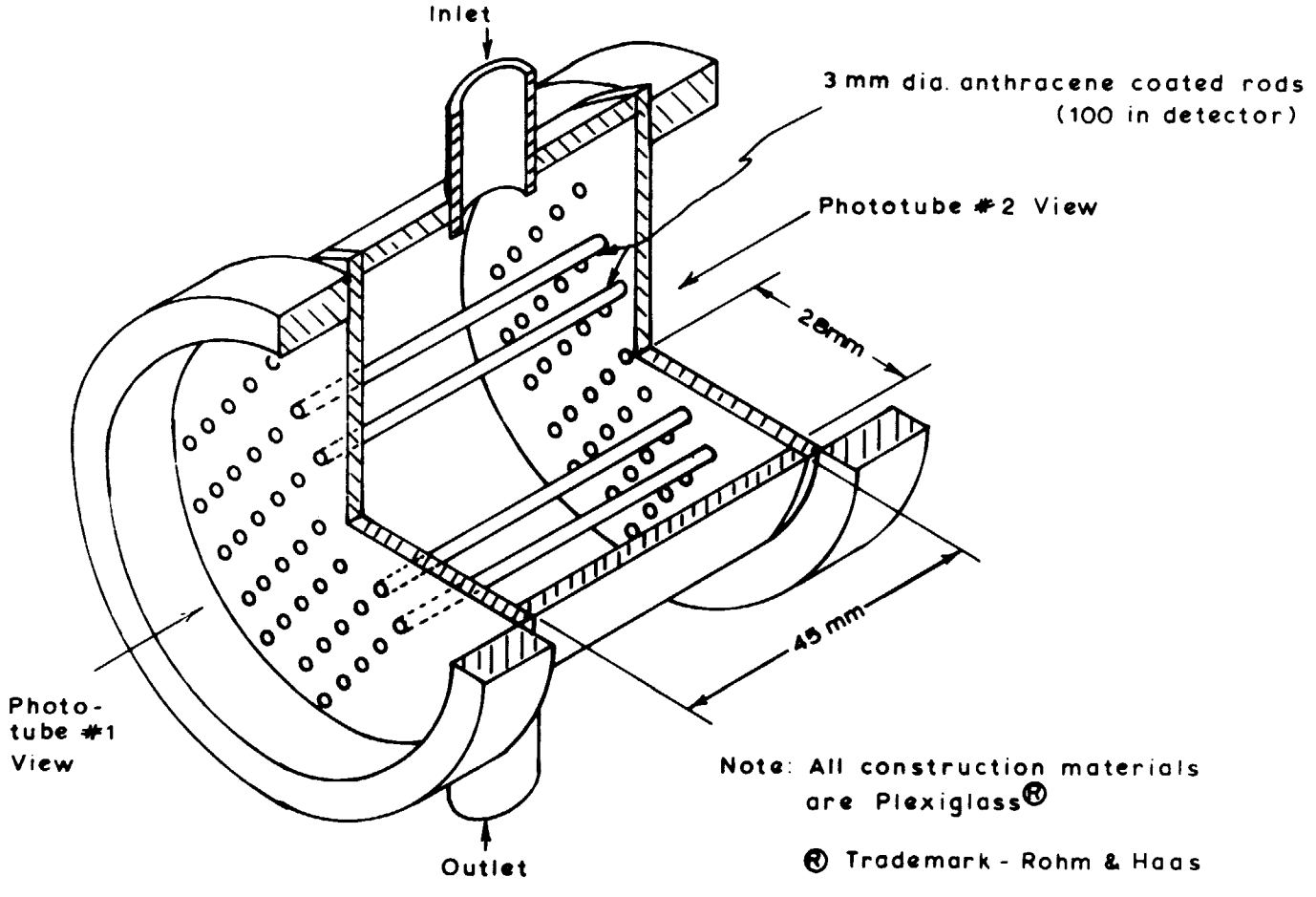

Figure 2. Schematic diagram of the scintillation detector.

are coated with anthracene by filling the assembled chamber with acetone and allowing it to remain for approximately ten minutes. The partially dissolved plexiglass forms a layer of adhesive upon which the anthracene is deposited by filling the chamber with powdered anthracene. The chamber is shaken for a few minutes and the excess anthracene is removed. It is probable that easier methods of detector production can be developed, e.g., precoating of rods.

The monitor was calibrated for the determination of tritium concentration in air with a device shown in Figure 3. Water of a known specific tritium activity was kept at a constant temperature in a bubbler. Air was passed through the bubbler for a certain length of time and the weight difference of the bubbler prior to and after the passage of air was compared to the volume of air passed through the detector.

It should be mentioned that the isotope effect as observed in the evaporation of tritiated water was disregarded. The presented results, in other words, should be regarded as conservative values inasmuch as the evaporated water has a lower specific activity than the original solution.

It was found that the response of the monitor was linear in the useful range, i.e., nCi/l and that a tritium concentration of one nCi/l of air corresponds to 20 counts per minute. The background of the monitor without shielding in the absence of gamma-emitting radionuclides was found to be 30 counts per minute.

It might be of interest to mention that this detector system may be used without alteration for monitoring of tritium in water and urine.

Although the described monitor was designed primarily for tritium

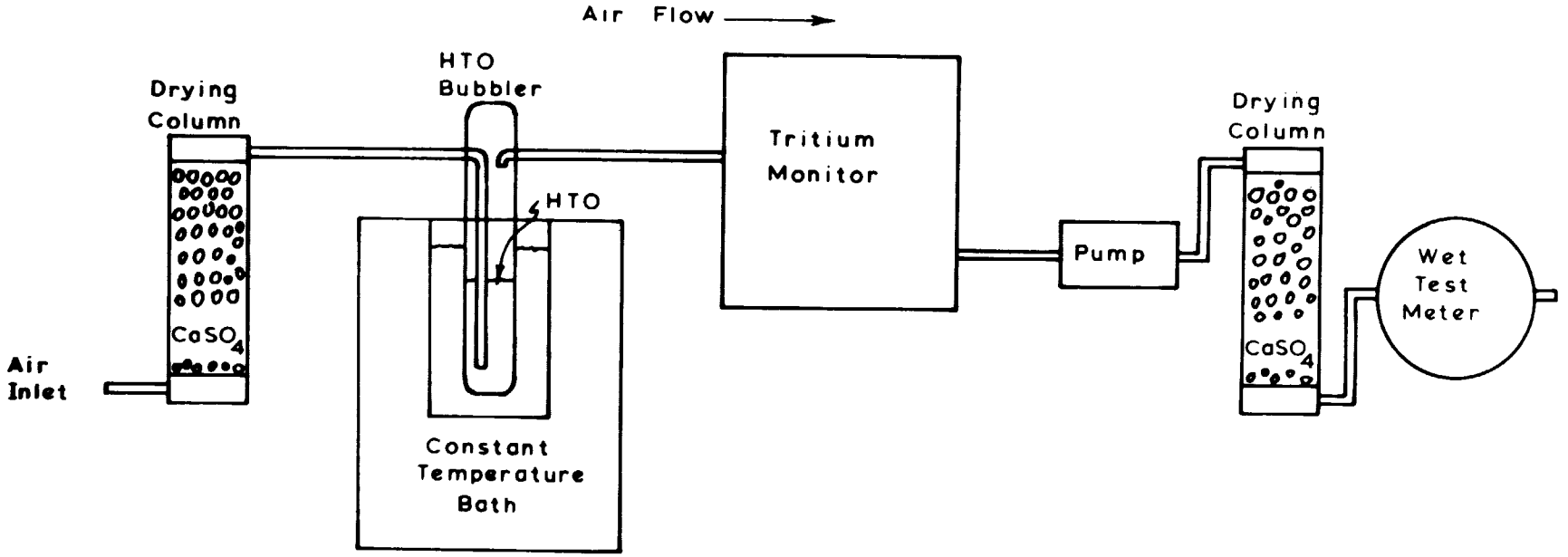

Figure 3. Device for laboratory calibration of tritium in air.

monitoring in air and water, other radionuclides may be detected under proper conditions. The monitor is presently being evaluated for ^{14}C and ^{85}Kr. Other investigations deal with improvements of the monitor. The optimum length of the detector and the thickness of anthracene coating is under study. The replacement of anthracene by calcium fluoride (Eu) and plexiglass by Teflon or glass make the detector applicable to monitoring of organic solvents and operable at elevated temperatures. An anticoincidence ring is under construction which would not only reduce the background in high-gamma fields, but would also make it possible to distinguish between beta and beta-gamma emitters in gaseous and liquid media.

Mention of commercial products used in connection with work reported in this article does not constitute an endorsement of the Public Health Service.

FIRST: The next paper which is number one on your sheet is entitled "Development of a Sampling Device for Distinguishing the Forms of Iodine in a Humid Atmosphere" by R. L. Bennett and R. E. Adams of the Oak Ridge National Laboratory. The speaker will be Mr. Bennett.

DEVELOPMENT OF A SAMPLING DEVICE FOR DISTINGUISHING THE FORMS OF IODINE IN A HUMID ATMOSPHERE*

By

R. L. Bennett and R. E. Adams

Reactor Chemistry Division, Oak Ridge National Laboratory, Oak Ridge, Tennessee

ABSTRACT

Analytical samplers, capable of distinguishing and measuring particulate, elemental and the less reactive iodine forms such as methyl iodide, are needed to aid in the assessment of the hazard of an accidental iodine release from a nuclear reactor and to predict its subsequent behavior. A major problem in the application of May pack iodine samplers has been the difficulty in finding the proper sequence of materials that will reproducibly separate the particulate iodine from elemental iodine. An improved sampler has been devised which contains a silver-plated aluminum inlet section that serves as a diffusion battery. The reactive molecular iodine is separated from aerosol particles due to its greater diffusivity. Test data to support this iodine sampling concept are presented.

INTRODUCTION

The high fission yield in nuclear reactors, its preferential release from over-heated fuel, and its significant biological hazard combine to make radioiodine one of the more important isotopes in the field of nuclear safety. To be able to assess the hazard of an accidental release of the iodine from a reactor, and to predict its subsequent behavior, one must have knowledge of the chemical and physical forms of the radioiodine. Iodine vapor may exist in the elemental form or be converted to volatile organic compounds by reaction with trace organic impurities on surfaces and in air. For example, methyl iodide has frequently been detected in containment studies involving fission product release from irradiated fuel. Radioiodine may also acquire the characteristics of a solid aerosol by adsorption onto the surface of fine particulate matter. Because the behavior of iodine in containment and the effectiveness of engineered safety systems, such as adsorbers, filters, and sprays, depends on the form of the iodine, analytical samplers are needed which are capable of distinguishing and measuring particulate, elemental and the less reactive iodine forms, such as methyl iodide, in experimental studies. F. G. May[1] of AERE developed a sampler which was designed to give physical and chemical information on iodine forms by filtration and preferential adsorption of iodine released in reactor containment experiments. This early "May pack" consisted of a brass-holder which contained

*Research sponsored by the U. S. Atomic Energy Commission under contract with the Union Carbide Corporation.

a Millipore filter, two charcoal-impregnated filter papers and a pack of 20 grams of granulated activated charcoal; particulate iodine was to be removed by the Millipore filter, elemental iodine by the charcoal-impregnated filter papers, and less reactive iodine forms (organic iodides) by the activated charcoal. Later modifications of the pack have included the placing of copper or silver-plated copper screens before the filters to remove reactive forms of iodine such as I_2.

This design and a number of variations have been employed by other workers and the samplers have been applied over wide ranges of humidity, temperature, and iodine concentration. In many cases, it is feared, the May packs were applied under conditions far removed from those under which the original pack was developed, while the response of the pack to the various iodine forms was interpreted, based upon May's earlier observations, without due regard for the effects of the new environment on the components of the pack. Because complete specificity of any pack component for removal of any one iodine form is not easily attainable, particularly over a wide range of conditions, it was felt necessary to establish the response of the pack under the conditions of application. Accordingly, a study was undertaken to test iodine samplers under conditions similar to those expected in the Loss-of-Fluid Test (LOFT) experiments with the purpose of documenting the response and also of determining the optimum components of the pack and their sequence within the pack.

TESTING PROCEDURE AND CONSTRUCTION OF CHARACTERIZATION PACKS

The tests were conducted at 90°C with a dry or 90% relative humidity air flow of one l/min through the packs. The testing facility is shown in Fig. 1 and the schematic flow diagram in Fig. 2. Filtered dry air passed at a low flow rate (30 ml/min) through the source U-tubes of iodine-131 labelled methyl iodide or elemental iodine or both. After mixing with a larger flow of dry air the stream joined a water-saturated air stream in the oven to make up the desired total flow and humidity. Because some variation occurs in the iodine sources, composite diffusion tubes were included in the tests to provide supplemental information as to the composition of each iodine source. The composite diffusion tube was of the standard arrangement found to be best[2] for iodine vapor characterization at high moisture conditions: a 30 cm silver-lined tube, a Drierite trap, a 30 cm rubber tube and a 20 cm charcoal-lined tube. In the earlier tests a composite diffusion tube (DT1) was placed in the sampling line at room temperature before the moisture was introduced. Another tube assembly (DT2) was placed parallel to the characterization packs (MP1 and MP2) in order to sample the stream under the same temperature and humidity conditions. As more experience was gained with the high humidity tube assembly (DT2) the use of the dry, room temperature tube (DT1) was discontinued.

An exploded view of an iodine characterization pack is shown in Fig. 3. The stainless steel hardware sections slide into the cylindrical aluminum holders which have an inserted stainless steel sleeve. The O-rings on the individual sections allowed flexibility in the component sequence so that testing alternative configurations was easily accomplished.

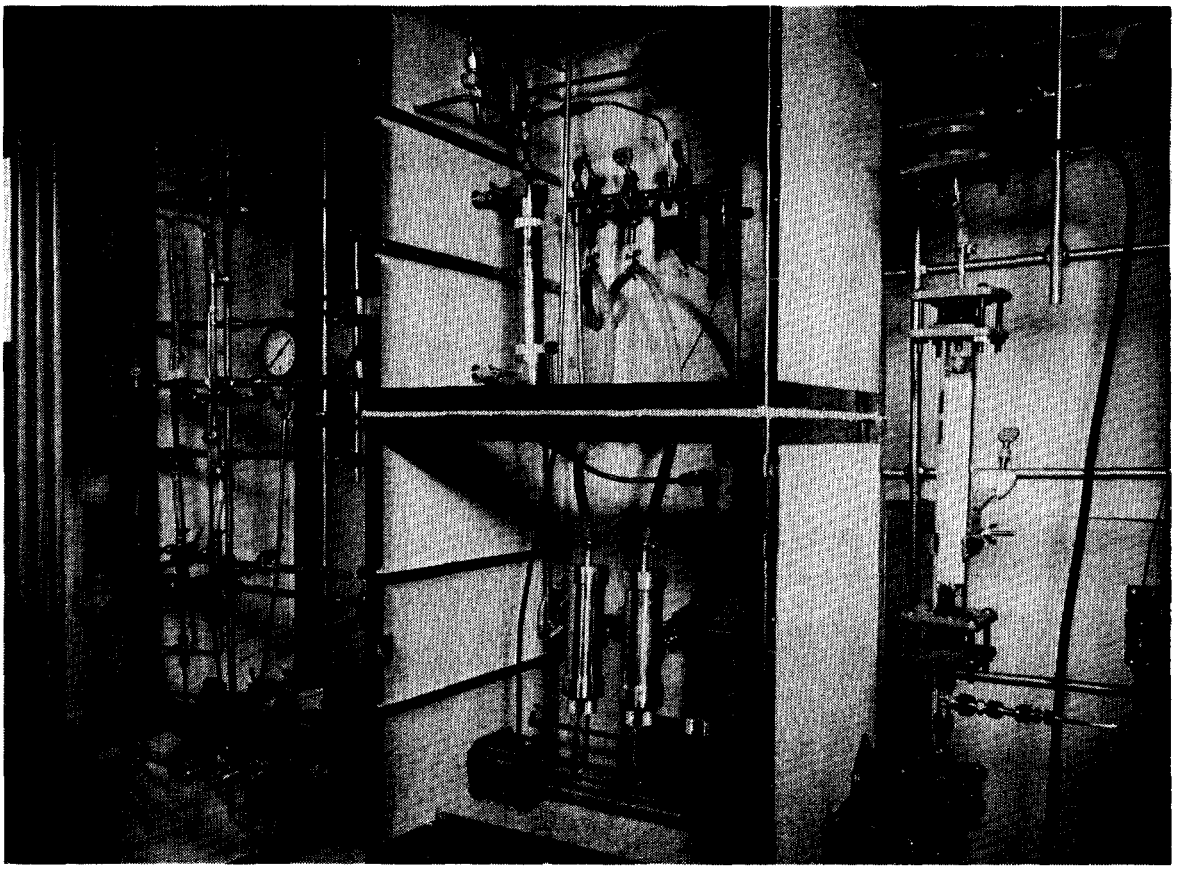

Figure 1

Testing Facility for Distribution of Iodine Species in Characterization Packs.

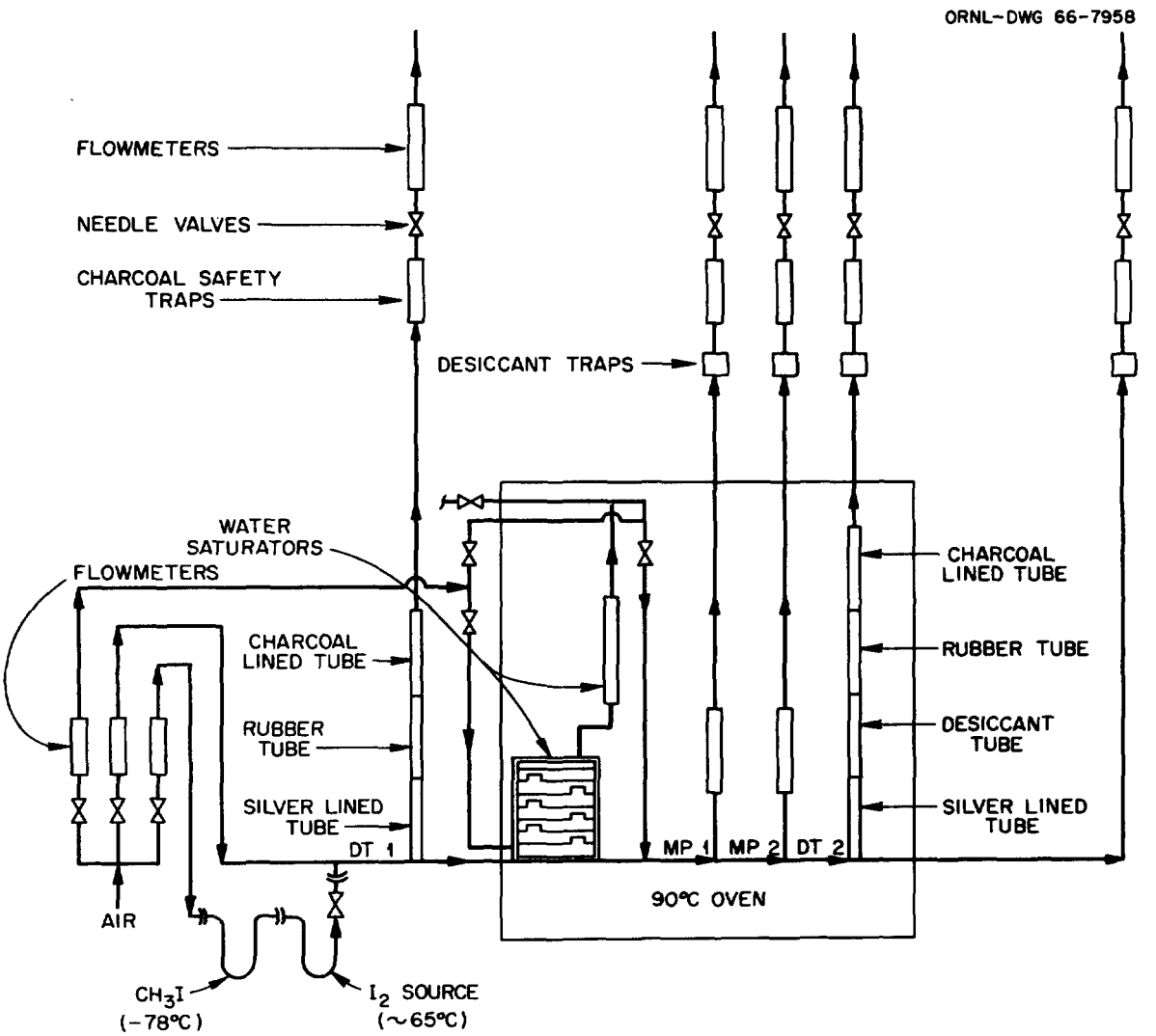

Figure 2

Flow Diagram of Characterization Pack Testing Facility.

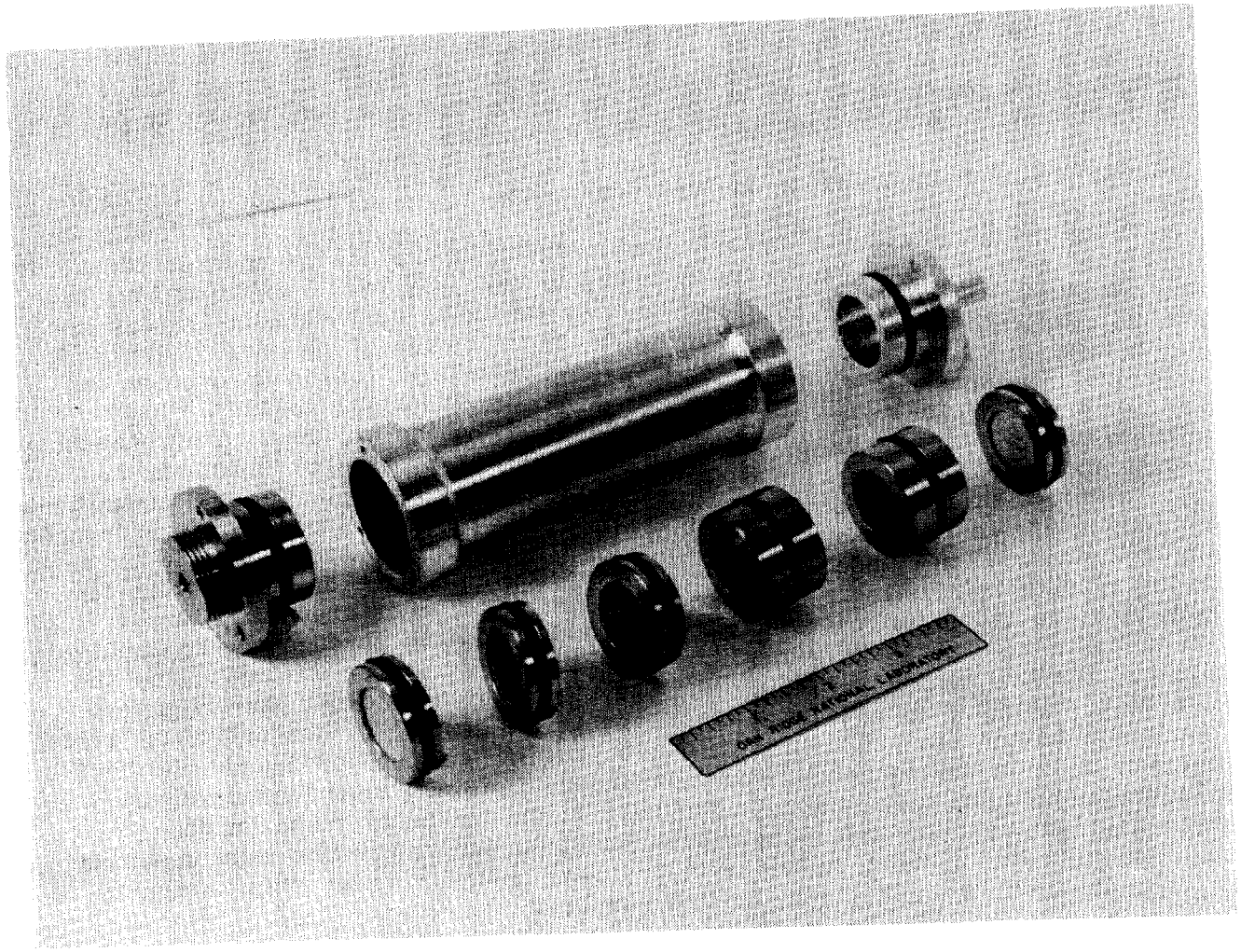

Figure 3

May Pack Proposed Initially for LOFT.

The pack arrangement examined first was that which was initially proposed by the LOFT program. The component sequence was: (1) a section of three high efficiency filters to remove particulate forms, (2) eight silver-plated screens to remove elemental iodine, (3) five charcoal-loaded filter papers for removal of easily adsorbed iodine compounds, (4) two 3/4-in. depth charcoal beds for adsorption of the more penetrating organic iodides such as methyl iodide and, finally (5) a high efficiency filter to remove airborne particles which might be eluted from the charcoal beds. Duplicate packs were assembled and installed, in parallel for each test as shown in Figs. 1 and 2. When each test was completed, the packs were completely disassembled and the radioactivity on each individual piece in each section was determined.

Distribution of Methyl Iodide on Pack Components

Since methyl iodide is the most penetrating of the iodine species identified in fission product release, the most commonly used May pack configurations have been designed with the intent that this compound will pass cleanly through the frontal components and be adsorbed in the charcoal beds at the end of the pack. It was necessary, therefore, to confirm that the methyl iodide adsorption on the preceding sections was negligible. Retention of methyl iodide by high efficiency filters was very small and should present no problem. The retention of methyl iodide on the various silver sections tested is shown in Table 1; the results indicate that reaction with silver poses no problem. Table 2 summarizes the adsorption of methyl iodide on charcoal-loaded filter paper which is designed to remove more easily adsorbed compounds but to allow the methyl iodide to pass into the charcoal bed which follows. The strong influence of humidity on the trapping of methyl iodide by the charcoal-loaded paper is shown in Fig. 4. Under dry conditions only about half of the CH_3I passed through the charcoal-loaded filters. The large variation noted in the amount of adsorption on the paper at the two humidity levels, and the observation by other investigators that CH_3I retention on this type of filter is influenced by contact time[3] leads to the conclusion that it is difficult to predict what proportion of the CH_3I activity will be trapped on charcoal loaded filter (ACG/B). Therefore, in application, it would be possible for iodine radioactivity found on the charcoal-loaded filter to be classified as a compound of iodine more reactive than methyl iodide, when, in actuality, it was methyl iodide; this ambiguity is not acceptable in an analytical iodine sampler.

In the May pack the organic iodide content of a gas sample should be found in the activated charcoal beds. In the early tests it was noted that, when a coconut charcoal (PCB) was used under humid conditions, some penetration of the first bed occurred. When an iodine-impregnated charcoal (MSA 85851) was employed, in later tests, the penetration of methyl iodide under humid conditions was eliminated (Table 3). This impregnated charcoal is also used in large-scale adsorbers for trapping methyl iodide, under humid conditions.[4]

Table 1. Retention of Methyl Iodide on Silver Screen Section

Test No.	Pack No.	CH_3I Load μg	Relative Humidity %	% Retention on Silver Section		
				8 Silver Screens	Hardware	Total
A	MP1	177.9	Dry	0.006	0.046	0.052
	MP2	159.1	Dry	0.010	0.044	0.054
B	MP1	37.3	90	0.009	0.056	0.065
	MP2	32.4	90	0.000	0.067	0.067

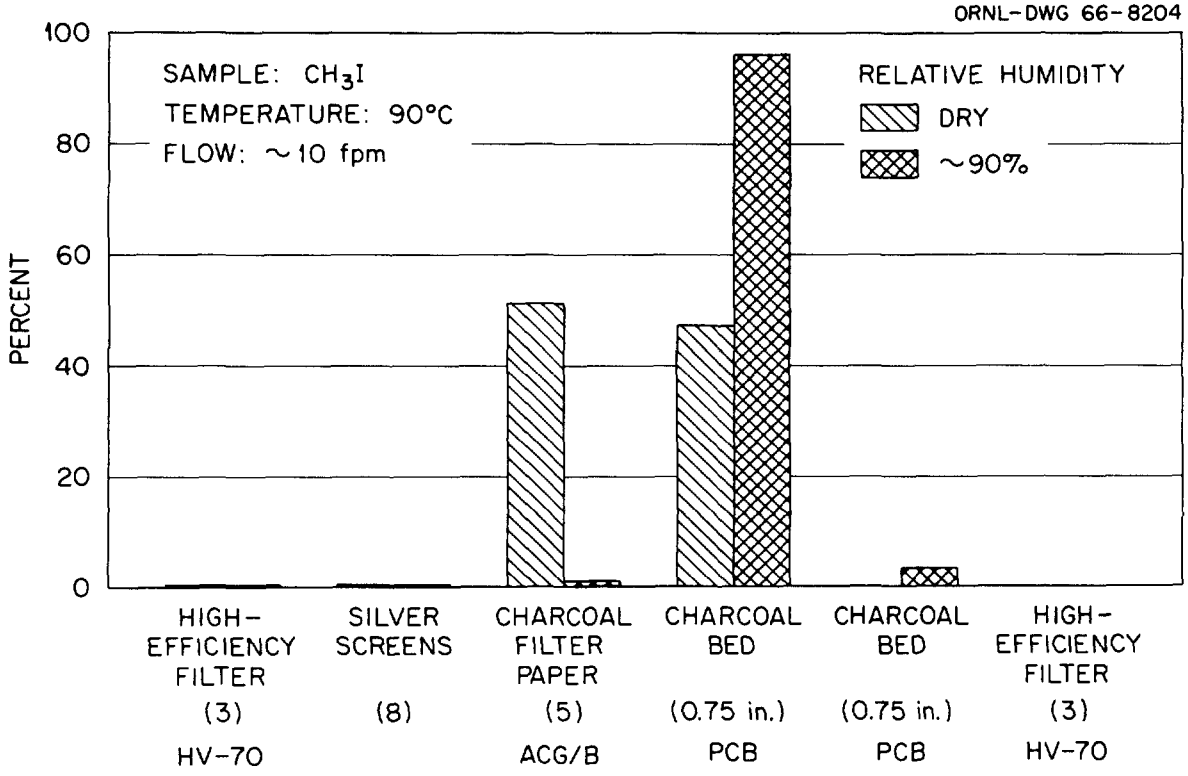

Figure 4

Distribution of Methyl Iodide from Dry and High Humidity Air Streams on Pack Components.

Table 2. Retention of Methyl Iodide by Charcoal Impregnated Filter Papers (ACG/B)

Test No.	Pack No.	CH_3I Load µg	% Relative Humidity	Flow Time min.	% Retention on 5 ACG/B Filters
A	MP1	178	Dry	5	58.53
	MP2	159	Dry	5	45.29
B	MP1	37.4	90	5	0.56
	MP2	32.5	90	5	0.70
G	MP1	7.8	90	10	0.40
	MP2	7.8	90	10	0.35
H	MP1	64.9	90	10	0.26
	MP2	64.7	90	10	0.26
P	MP1	82.7	90	10	7.73
	MP2	79.6	90	20	8.20
Q	MP1	29.5	90	10	1.13
	MP2	31.9	90	20	0.82
V	MP1	13.1	90	10	21.96
	MP2	12.5	90	20	23.92

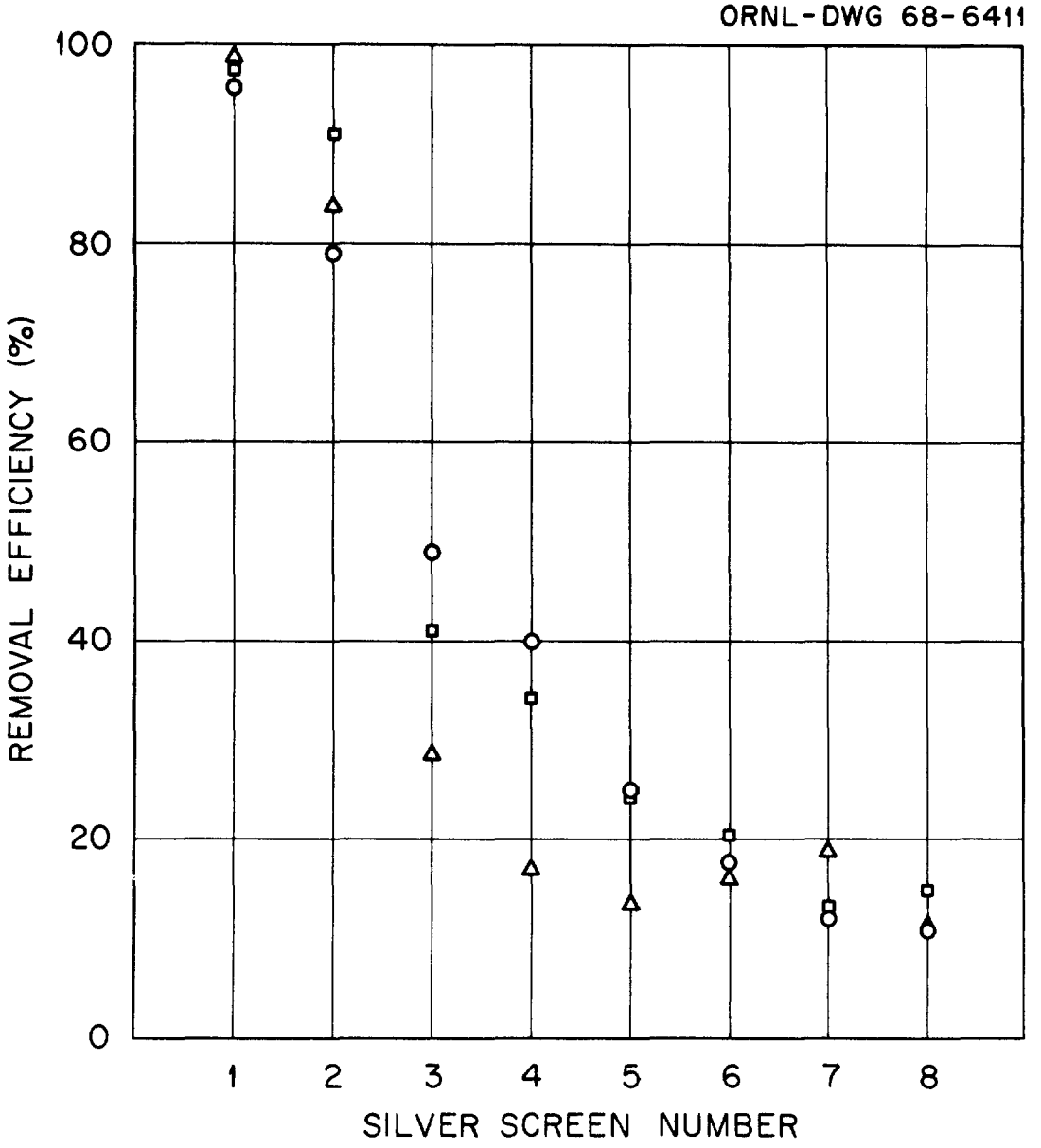

Figure 5

Decrease in Individual Efficiency of Silver Screens As Iodine Passes Through 8-Screen Section.

Table 3. Methyl Iodide Penetration of First Charcoal Bed

Test No.	Pack No.	Charcoal Type	Relative Humidity %	% Penetration of First Charcoal Bed
A	MP1	PCB 12/30	Dry	0.00
	MP2	PCB 12/30	Dry	0.00
B	MP1	PCB 12/30	90	1.82
	MP2	PCB 12/30	90	3.34
G	MP1	PCB 12/30	90	12.30
	MP2	PCB 12/30	90	9.27
H	MP1	PCB 12/30	90	10.46
	MP2	PCB 12/30	90	9.62
P	MP1	MSA 85851	90	0.00
	MP2	MSA 85851	90	0.01
Q	MP1	MSA 85851	90	0.02
	MP2	MSA 85851	90	0.02

Distribution of Elemental Iodine on Characterization Pack Components

If the choice in separation of particulate iodine from iodine vapors is by filtration of the particles, then it is essential to have a high efficiency filter material which retains little elemental iodine or at least only moderate, reproducible amounts. A summary of the retention values of elemental iodine on a large number and types of filters is presented in Table 4. None of the filters look attractive for this separation process. Some of the filter materials such as HV-70 removed almost all of the iodine and, while others did hold much smaller percentages, none appeared to be reproducibly small. The most promising one appeared to be Zitex, a porous TFE membrane filter, but with this material there is still the problem of adsorption on the supporting hardware. Also, radiation damage to Teflon may be sufficient to preclude its use.

The purpose of this silver component is to remove reactive iodine such as elemental iodine and hydrogen iodide and allow nonreactive forms such as methyl iodide to pass. The desirable low retention of the latter has been confirmed (Table 1) and discussed. If the alternative sequence in which the silver section precedes the high efficiency section is employed, then particles must also pass through the section. This is discussed in the next section on aerosol removal.

Two types of silver components used in conventional May pack designs have been tested for elemental iodine adsorption: eight 80-mesh silver-plated screens and two Flotronics silver membrane (5 micron pore) filters. The efficient removal of both of these types is shown in Table 5. With silver screens a decrease in the removal efficiency was found as the iodine passes through the successive screens(Fig. 5). When this is replotted in terms of the log of the incident iodine load to each screen versus the removal efficiency (Fig. 6), a linear decrease in efficiency was observed below about 10 micrograms. This behavior, which is similar to that observed by Keller, Duce and Cartan[5] on series of silver membranes, may be due to less reactive impurities which become more significant as the amount of incident elemental iodine decreases.

Retention of Irradiated Stainless Steel-UO_2 Aerosol on Screens

The alternative characterization pack arrangement in which elemental iodine is separated from particles and non-reactive vapor forms consists of a silver component followed by a high efficiency filter section. To be effective only small amounts of particulate material may adhere to the silver. Removal efficiencies were determined using an aerosol facility in which radioactive particles were generated by arc-melting irradiated stainless steel tubes with a UO_2 insert and passed through the tested component which was backed up with efficiency filters. The high aerosol removal by the eight 80-mesh screens (Table 6) apparently precludes the use of this type section.

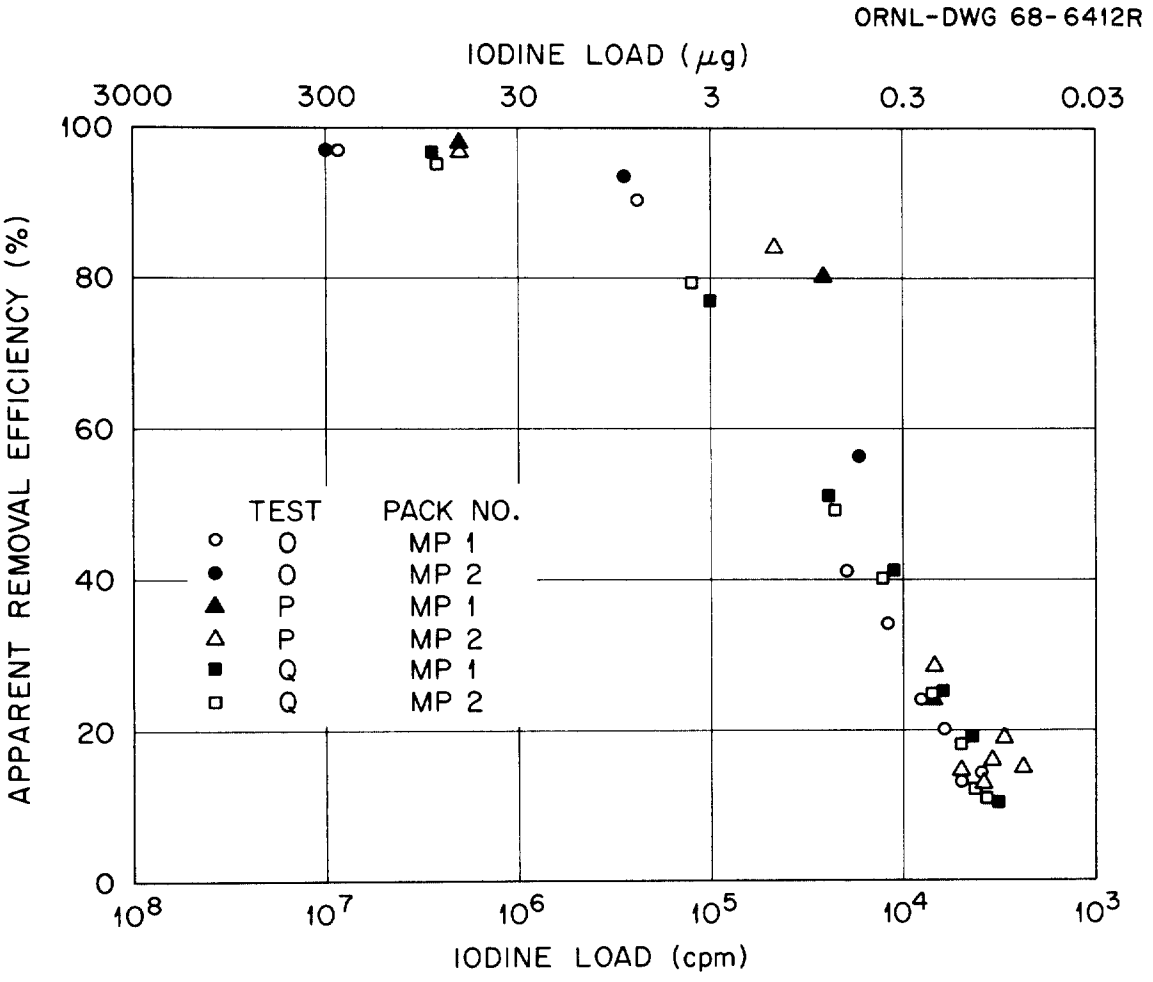

Figure 6

Apparent Efficiency for Elemental Iodine Removal as Load on Silver Screens Decreases.

Table 4. Removal of Elemental Iodine by Various Types of High Efficiency Filters (90°C, 90% Relative Humidity)

Test No.	Pack No.	Filter Material	Iodine Load μ	% I_2 Removal 3 Filters	Hardware	Total
D	MP1	HV-70	135.4	96.99	2.69	99.68
	MP2	HV-70	116.8	95.82	3.44	99.26
F	MP1	AP-20	235.0	10.40	7.69	18.09
	MP2	AP-20	234.4	10.70	4.60	15.30
G	MP1	F-700	41.2	4.54	4.49	9.03
	MP2	F-700	37.8	4.78	4.32	9.10
H	MP1	F-700	23.4	41.65	20.21	61.86
	MP2	F-700	21.5	46.52	24.00	70.52
J	MP1	F-700	19.3	38.78	23.06	61.84
	MP2	F-700	18.8	35.59	27.92	63.51
K	MP1	C1G	20.8	91.01	7.64	98.65
	MP2	C1G	14.3	92.78	5.32	98.10
	MP3	C1G	10.1	94.47	3.28	97.75
L	MP1	F-700	13.1	74.57	19.79	94.36
	MP2	C1G	14.9	88.30	9.51	97.81
	MP3	934AH	9.2	98.20	9.23	96.43
N	MP1	Zitex (5-10 micron pore)	182.0	2.56	10.14	12.70
			225.1	1.86	18.92	20.78
R	MP1	Zitex (5-10 micron pore)	127.7	2.62	6.27	8.89
			112.8	2.56	6.00	8.56
S	MP1	Gelman "A"	217.1	41.35	12.00	53.35
	MP2	Gelman "A"	203.7	47.52	10.91	58.43

Table 5. Removal of Elemental Iodine by Silver Components from 90°C, 90% Relative Humidity Air

Test No.	Pack No.	Iodine Load µg	% Iodine Removal		
			Silver Component	Hardware	Total
8 Silver Screens					
O	MP1	66.0	98.75	1.01	99.76
	MP2	66.3	93.26	6.44	99.70
P	MP1	73.3	88.92	10.84	99.76
	MP2	70.1	90.16	9.68	99.84
Q	MP1	85.9	98.07	1.79	99.86
	MP2	82.0	96.68	3.18	99.86
2 Silver Membrane Filters					
R	MP1	127.7	96.97	2.49	99.46
	MP2	112.8	98.14	1.22	99.35

Table 6. Retention of Aerosols on Pack of 8-80 Mesh Screens

Test No.	% Relative Humidity	Flow l/min	% Retention		
			Screens	Hardware	Total
CS1	25-33	1	76.9	13.8	90.7
CS2	25-33	1	73.9	9.5	83.4

DEVELOPMENT OF HONEYCOMB IODINE SAMPLER

The poor separation results obtained in the tests (1) with a high efficiency filter section and (2) with a silver section in the first position of the packs led to the development of a sampler containing a silver honeycomb as the initial section. The use of the silver honeycomb is based on the principle that molecular size particles have much larger diffusion coefficients than larger particulate matter. Elemental iodine has a diffusivity of about 0.1 cm^2/sec in dry air at room temperature which may be compared with the submicron particles shown in Fig. 7 which were calculated by Browning and Ackley.[6]

The function of particles removed by deposition on the walls of a cylindrical diffusion channel is given by equations derived by Gormley and Kennedy:[7]

$$E = 1 - F = 1 - (0.819e^{-3.657\mu} + 0.097e^{-22.3\mu} + 0.032e^{-57\mu}) \quad (1)$$

$$E = 2.56\mu^{2/3} - 1.2\mu - 0.177\mu^{4/3} \quad (2)$$

where

$E = 1 - F$ = fraction of particles removed

$F = N_g/N_o$ = fraction of particles penetrating the channel

N_g = number of particles remaining in gas

N_o = number of particles entering the channel

$\mu = \pi DZ/Q$

D = diffusion coefficient of particles in carrier gas, cm^2/sec

Z = distance from channel entrance, cm

Q = volumetric flow rate of carrier gas, cm^3 sec.

It is assumed that once a particle diffuses to the channel wall, it adheres. The derivation of Eq. (1) assumed that the concentration of particles falls continuously along the axis of the channel and from the axis to periphery, that is, there are conditions of steady diffusion toward the walls. It should be used for values of μ greater than 0.3. For smaller values of μ these conditions are not established and Eq. (2) is applicable. Thomas[7] has derived a single equation which yields values of E agreeing with (1) and (2) within 0.001 for all values of μ:

$$E = 1 - (0.819e^{-3.657\mu} + 0.097e^{-22.3\mu} + 0.032e^{-57\mu} + 0.027e^{-123\mu} + 0.025e^{-750\mu}) \quad (3)$$

Calculated Diffusion Coefficients for Submicron Particles in Air (Browning and Ackley[6]).

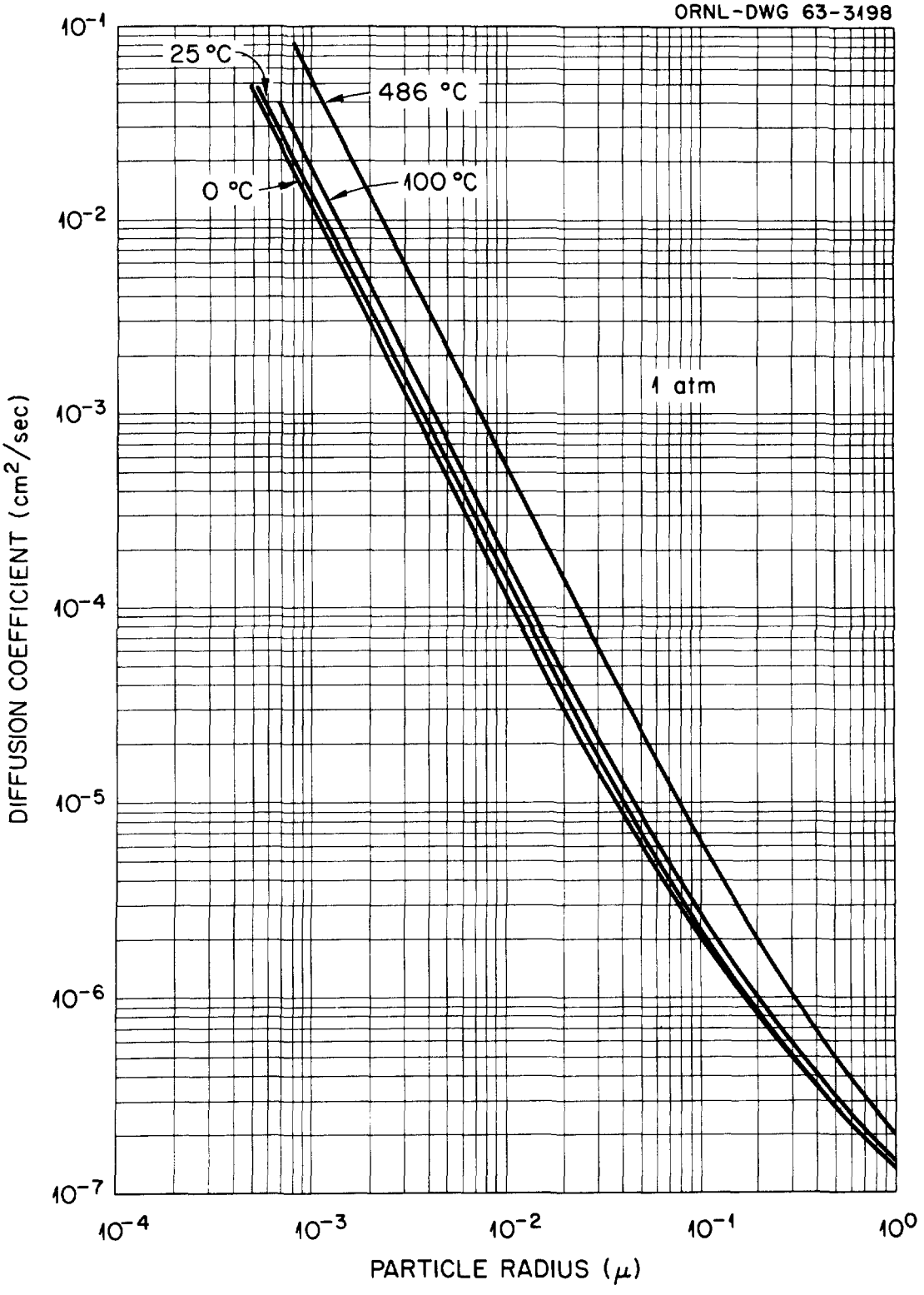

Figure 7

A plot of the retention of particles on the wall of a cylindrical tube versus the dimensionless group, μ, is shown in Fig. 8.

The deposition per unit length of channel, n_s, may be found by differentiation of Eq. (3) with respect to length. For values of μ greater than about 0.3, only the first term is significant and the following relationship is obtained.

$$n_s = \frac{\partial N_g}{\partial Z} = \frac{N_o D}{Q} (9.41\ e^{-11.49\ DZ/Q}) \qquad (4)$$

From this equation it can be shown that

$$(\Delta \log n_s/DZ) = 5.00\ D/Q. \qquad (5)$$

If the log of the deposition per unit length is plotted against the distance from the tube entrance, a straight line should be obtained. The diffusion coefficient may be calculated from the slope of this line.

The honeycomb offers an ideal geometry since it divides a large total volumetric flow required for sampling low concentrations into smaller parallel flows which are needed for deposition on short lengths. At the same time the honeycomb presents a minimal cross-section so that other particle collecting mechanisms such as interception and inertial impaction are small. The proposed honeycomb characterization pack, shown in Fig. 9, consists of a 5 cm silver-plated honeycomb with 1/8-in. hexagonal channels followed by a high efficiency filter section for aerosol removal and an impregnated charcoal bed for methyl iodide adsorption. This honeycomb has been tested (Table 7) with methyl iodide, elemental iodine and aerosols individually. About 99.7% of the elemental iodine was retained on the honeycomb whereas only about 1% or less of the methyl iodide was adsorbed and only about 1-2% of the aerosol stuck to the 5 cm honeycomb.

In the elemental iodine tests the lower efficiency of Test T was due to lack of dispersion of the iodine entering the pack through all of the hexagonal channels. It was observed by visual examination and radioactivity counting that most of iodine travelled down the center third of the honeycomb. By increasing the inlet diameter and tapering the section opening out to the diameter of the honeycomb, the distribution was improved and the higher efficiencies were observed. The distribution of deposited iodine activity on the honeycomb was determined by flattening the section and cutting it into five 1 cm lengths. As seen in Fig. 9 a plot of the log of the deposited activity on each section versus its distance from the entrance yielded a straight line. In this test a 30 cm diffusion tube was placed parallel to two honeycomb samplers. From the diffusion tube data an apparent diffusion coefficient of 0.13 cm^2/sec was calculated for the iodine at the 90°C, 90% relative humidity conditions. Using this coefficient, the relative flows in the two devices and the assumption that the deposition on the hexagonal channels is the same as that on cylindrical tubes having the same cross-section, the theoretical slope shown in Fig. 10 was calculated. The experimental deposition on the honeycomb agrees well with this calculated slope.

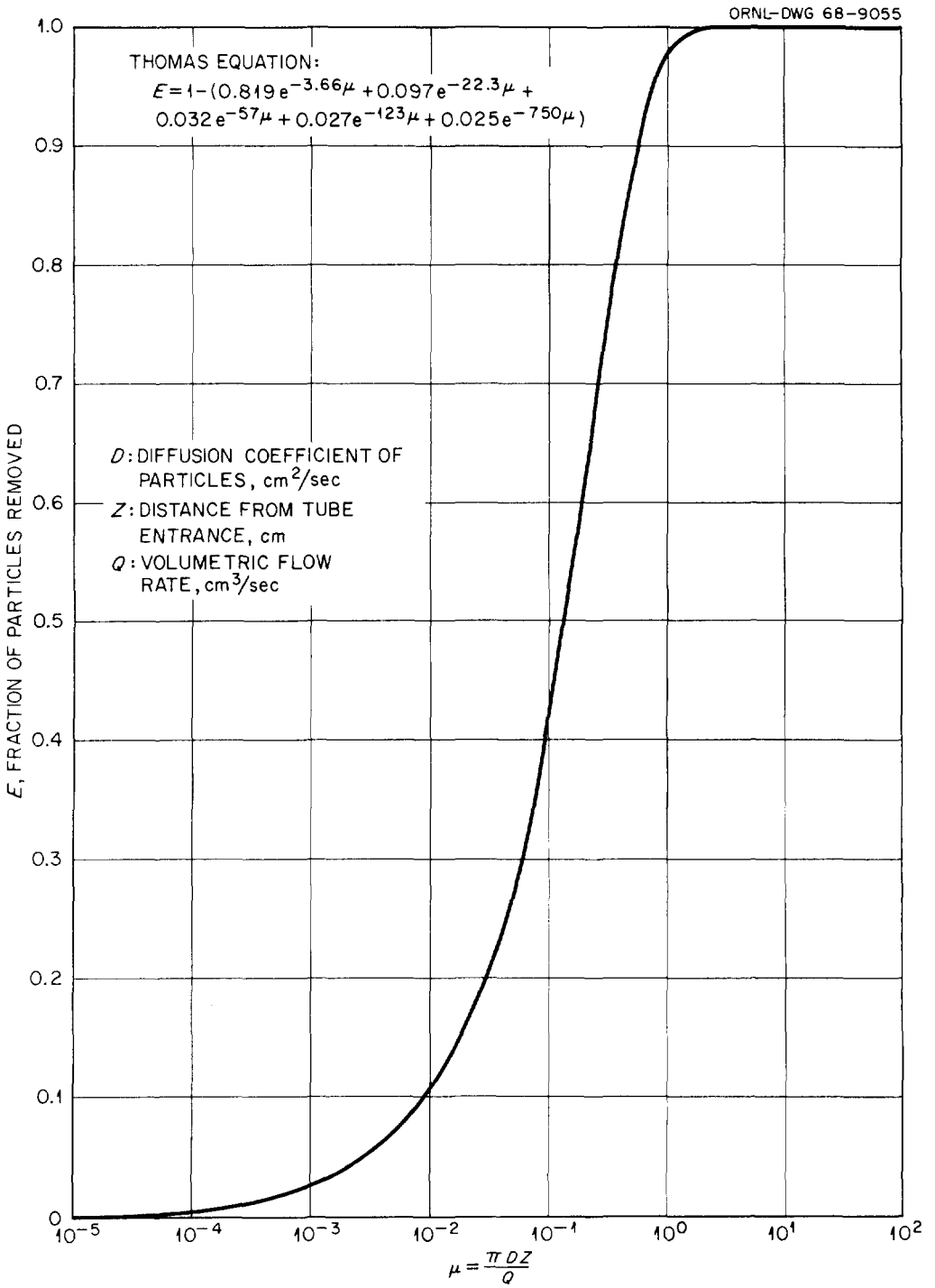

Figure 8

Removal of Particles by Diffusion in Cylindrical Tubes

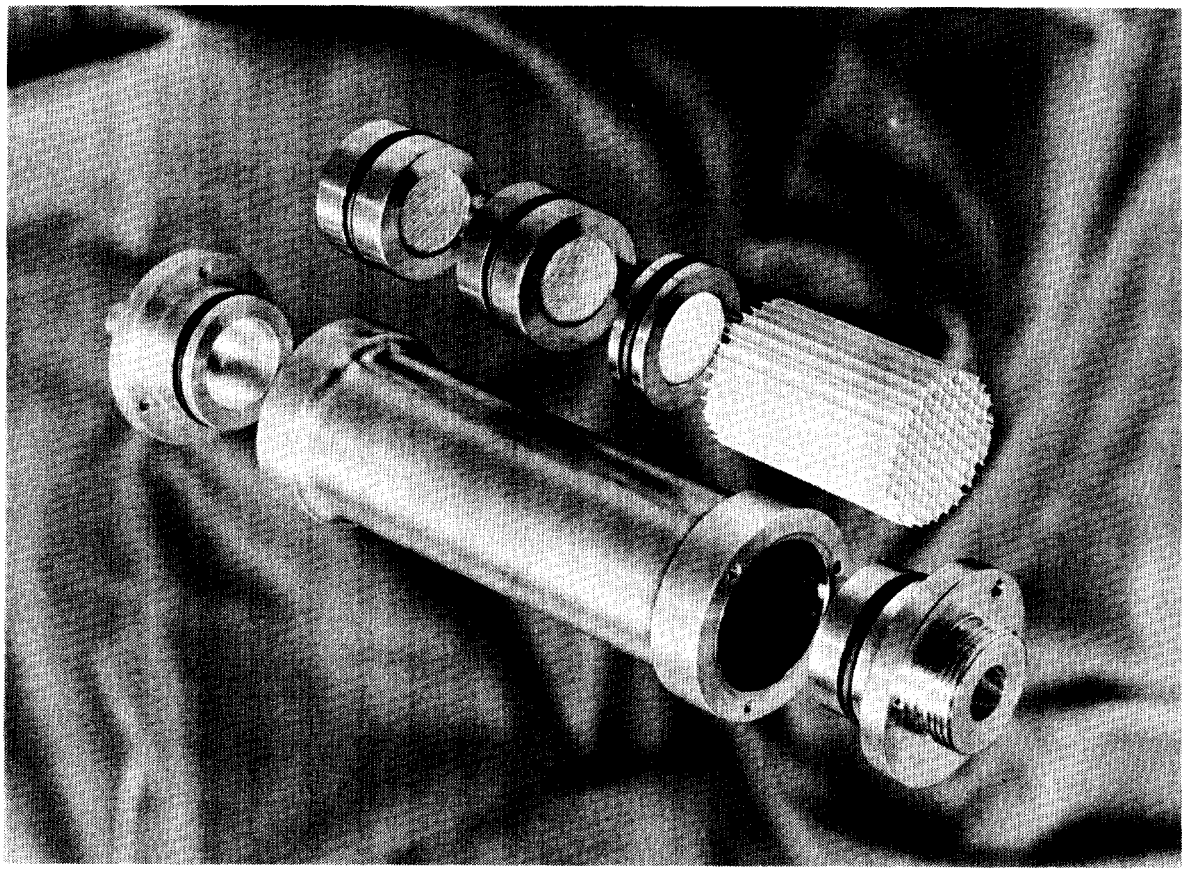

Figure 9

Iodine Sampler with Silver Honeycomb.

Diffusional Deposition of Elemental Iodine in 30 cm Silver Tube and a 5 cm Silver Honeycomb Section.

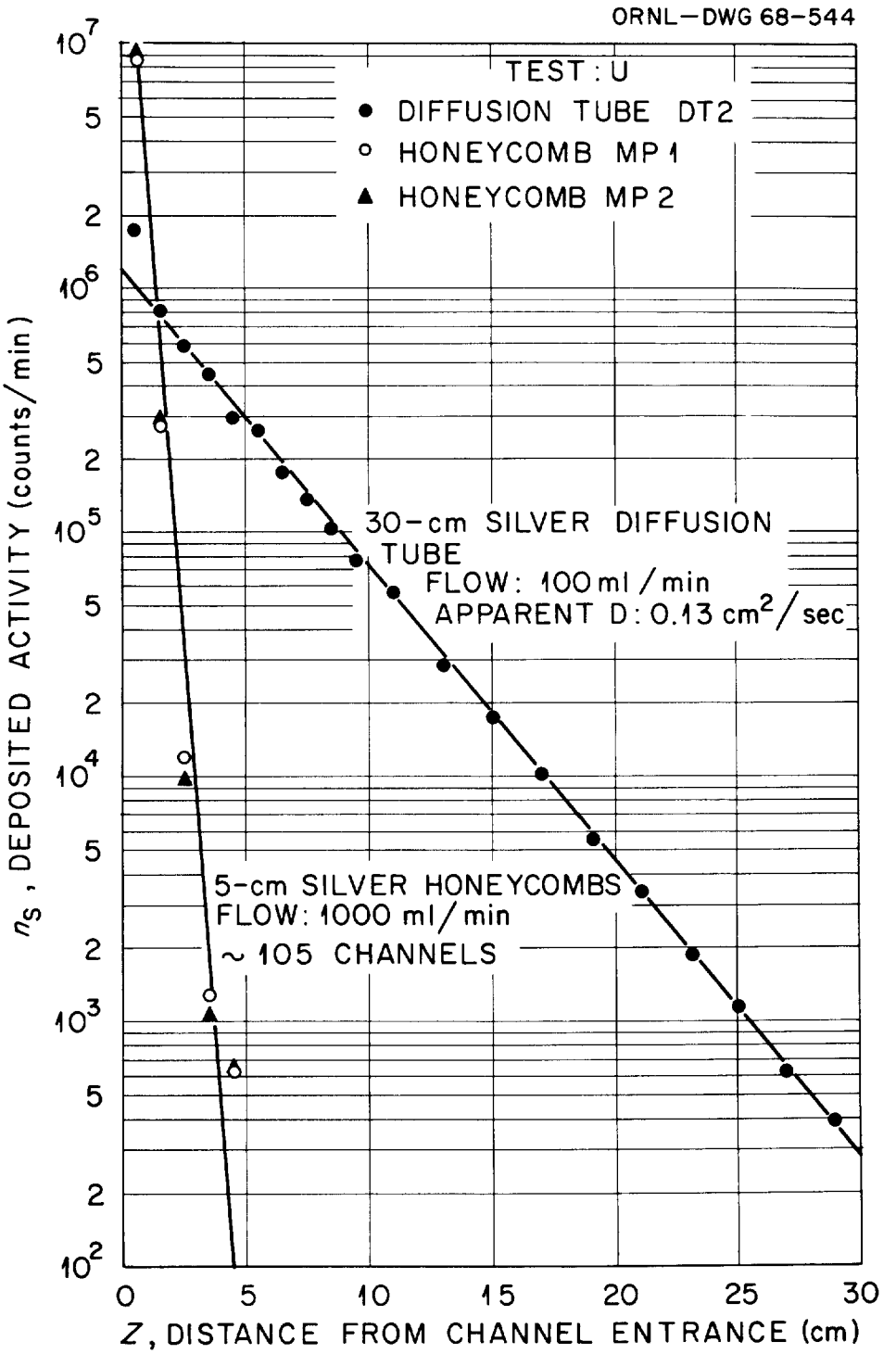

Figure 10

An additional test has been made in which a mixture of elemental iodine and irradiated stainless steel-UO_2 aerosol was introduced into a 0.1 m^3 tank, aged 10 min, and then passed through honeycomb samplers. The results as shown in Table 8 confirmed the excellent separation. The small amount (approximately 1%) of the radioiodine which penetrated to the charcoal bed probably resulted from conversion of elemental iodine to methyl iodide.

The observed low retention (about 1%) of aerosol on the 5 cm honeycomb, combined with the high removal efficiency for elemental iodine, indicate that the silver honeycomb is the most effective device for separation of the two which we have examined.

Additional testing has been conducted with the honeycomb sampler. Surface contamination of the silver prior to use,with a possible drop in removal efficiency, was considered. One possible source of contamination is reaction of the silver with sulfides in the air (tarnishing). An extreme test of this was made by passing hydrogen sulfide through a silver honeycomb to produce a coverage of silver sulfide. From an economic standpoint the deposition of iodine on a bare unplated aluminum honeycomb was of interest. Three iodine samplers containing a fresh silver-plated honeycomb, a silver sulfide coated honeycomb and an unplated aluminum honeycomb, respectively, were exposed to a 90°C, 90% relative humidity air stream containing elemental iodine. The distributions of the deposited iodine on the three samplers are shown in Table 9. The honeycomb with the sulfide surface was only very slightly less efficient for iodine removal than the fresh silver honeycomb. The penetration of a large fraction of the iodine through the aluminum honeycombs shows that reaction is not complete and the bare, unplated aluminum is not satisfactory for this purpose.

CONCLUSIONS

After extensive testing of a large variety of high efficiency filters no type has been found which consistently exhibits low elemental iodine adsorption. If a filter which would remove no elemental iodine were available, there remains the problem of iodine adsorption on the hardware which holds the filter. Another disadvantage of this arrangement is the possibility that as particulate matter deposits on the filter during sampling, these particles may adsorb iodine. For these reasons the sampler arrangement with an elemental iodine removing (silver) section first is recommended.

The recommended silver component is a silver-plated honeycomb of the proper dimensions to ensure iodine removal at the sampling flow rate. The difficulty in interpreting the distribution of methyl iodide between the charcoal-loaded filter paper section and charcoal bed makes the value of the charcoal filter paper section questionable. Use of iodine-impregnated charcoal is recommended in the charcoal bed for maximum retention of methyl iodide.

In summary, the sequence we have found to be the most useful for iodine characterization is: silver honeycomb for elemental iodine removal, three high

Table 7. Retention of Elemental Iodine and Penetration of Methyl Iodide and Stainless Steel Aerosol in Separate Tests with Honeycomb Section

Species	Test	Pack No.	Load, μg	% Relative Humidity	% Retention on Honeycomb
I_2	T	MP1	386	90	97.68
		MP2	397	90	97.79
	U*	MP1	340	90	99.81
		MP2	306	90	.61
	X*	MP1	1052	100	99.75
		MP2	1038	100	99.65
CH_3I	V*	MP1	13.1	90	0.92
		MP2	12.5	90	1.34
	Y*	MP1	131	100	0.59
		MP2	154	100	0.48
Aerosol	HC1			~ 15	2.27
	HC2			~ 91	0.71
	HC3			~ 95	0.73

*Inlet hardware modified between tests T and U to provide more uniform distribution of air flow through honeycomb.

Table 8. Percentage Distribution of Elemental Iodine-Aerosol Mixtures Through Characterization Packs

	Elemental Iodine (^{131}I)		Aerosol (^{51}Cr)	
	Pack 1	Pack 2	Pack 1	Pack 2
Honeycomb				
1st cm	92.97	93.02	$\leq$ 1.0	$\leq$ 0.7
2nd cm	4.18	4.31	$\leq$ 0.30	$\leq$ 0.14
3rd cm	1.13	0.75	$\leq$ 0.15	$\leq$ 0.12
4th cm	0.34	0.24	$\leq$ 0.10	$\leq$ 0.10
5th cm	0.17	0.15	$\leq$ 0.10	$\leq$ 0.10
Total	98.78	98.47	$\leq$ 1.65	$\leq$ 1.16
Filters				
3 Gelman A	0.04	0.07	$\geq$ 98.2	$\geq$ 98.6
Silver	0.22	0.16	$\leq$ 0.03	$\leq$ 0.07
Total	0.26	0.23	$\geq$ 98.2	$\geq$ 98.7
Charcoal Bed	0.95	1.30	$\leq$ 0.14	$\leq$ 0.15

Table 9. Distribution of Elemental Iodine on Individual Characterization Packs with Silver, Silver Sulfide and Aluminum Honeycombs

	Type of Honeycomb		
	Silver	Silver Sulfide	Aluminum
Honeycomb			
1st cm	96.24	93.17	33.77
2nd cm	3.33	5.92	11.69
3rd cm	0.22	0.38	7.07
4th cm	0.02	0.05	5.27
5th cm	0.01	0.03	10.02
Total	99.82	99.55	67.82
Filters			
3 Gelman A	0.13	0.27	13.34
1 Flotronics Silver	0.00	0.04	18.24
Hardware	0.00	0.00	0.31
Total	0.13	0.31	31.58
First Charcoal Bed	0.05	0.14	0.27
Second Charcoal Bed	0.00	0.00	0.01

efficiency filters for particulate removal, two iodine-impregnated charcoal beds, and finally three high efficiency filters for stopping airborne particles from the charcoal bed. The iodine which is on the particles that stop on the first high efficiency filter section may be reversibly adsorbed so the use of a silver membrane filter as the last layer in the section is suggested. With all iodine samplers, some of the elemental iodine "plates out" on almost any surface available to it before it enters the silver component of the sampler. If the analysis obtained from the sampler is to be representative of the environment which it samples, the inlet hardware surface should be minimal. The activity deposited on this surface probably should be included with that which deposits on the silver component in determining the total reactive molecular iodine.

ACKNOWELDGEMENTS

The authors wish to acknowledge and express their appreciation to J. Truitt and J. S. Gill for their assistance with the aerosol tests.

REFERENCES

1. W. J. Megaw and F. G. May, Jr., "The Behavior of Iodine Released in Reactor Containers," Reactor Sci. Tech. (J. Nucl. Energy Parts A/B) 16, 427 (1962).

2. R. E. Adams, R. L. Bennett, and W. E. Browning, Jr., Characterization of Volatile Forms of Iodine at High Relative Humidity by Composite Diffusion Tubes, ORNL-3985, Oak Ridge National Laboratory, August 1966.

3. R. E. Davis and Mrs. J. M. E. Williams, The Efficiency of Whatman Type ACG/B Filter Papers for Methyl Iodide Retention in Air, British Report AEEW-M-568, November 1965.

4. R. D. Ackley, R. E. Adams, W. E. Browning, Jr., G. E. Creek and G. W. Parker, "Retention of Methyl Iodide by Charcoal Under Accident Conditions," Nuclear Safety Program Semiannual Progress Report December 31, 1965, ORNL-3915, Oak Ridge National Laboratory, pp. 61-80.

5. J. H. Keller, F. A. Duce, and F. P. Cartan, Retention of Iodine on Selected Particulate Filters and a Porous Silver Membrane Being Considered for the LOFT May Pack, IN-1078, Idaho Nuclear Corporation, May 1967.

6. W. E. Browning, Jr. and R. D. Ackley, "Decontamination Factors for Particle Deposition in Containment Vessel Leaks," Nuclear Safety Program Semiannual Progress Report June 30, 1965, pp. 39-40, Oak Ridge National Laboratory, ORNL-3483.

7. J. W. Thomas, "Particle Loss in Sampling Conduits," Proceedings of Symposium on Instruments and Techniques for Assessment of Airborne Radioactivity in Nuclear Operations, IAEA, Vienna, 1967.

8. P. G. Gormley and M. Kennedy, "Diffusion from a Stream Flowing Through a Cylindrical Tube," Proc. Roy. Acad. Sci. A-52, 163-169 (1949).

DISCUSSION

VILES: Is this pure silver or silver plated?

BENNETT: It was silver plated aluminum.

FIRST: The next paper is entitled "Radioactive Aerosol Size Classification Experience with a Low Pressure Cascade Impactor" by G. W. Parker, H. Buchholz and W. J. Martin of Oak Ridge National Laboratory. Dr. Parker will make the presentation.

RADIOACTIVE AEROSOL SIZE CLASSIFICATION EXPERIENCE WITH A LOW PRESSURE CASCADE IMPACTOR*

G. W. Parker, H. Buchholz[/] and W. J. Martin

Reactor Chemistry Division
Oak Ridge National Laboratory
Oak Ridge, Tennessee

ABSTRACT

Aerosol particles in the submicron range are expected to be released from overheated reactor fuel materials as indicated in numerous experiments which simulate reactor accidents resulting from a loss-of-coolant. Devices to measure aerodynamic particle size in the submicron region are therefore required and a simple, passive, nearly foolproof device is particularly desirable. In this work an improvement on a standard instrument, an inertial impactor, which operates at subatmospheric pressure thereby increasing both the mean free path of the air molecules and the Cunningham correction (for the slip of small particles between gas molecules) was conceived and investigated to test this principle.

A commercially available Andersen Impactor was first successfully modified for low pressure operation to extend its range to submicron sizes and then an impactor of original design was built, tested and calibrated. The useful range of the new instrument was found to be from less than 0.01 micron to several microns particle diameter. The range is variable and is dependent upon the selected operating pressure. The impactor is assembled and disassembled quickly and employs throw-away impactor plates to facilitate radiochemical analysis and decontamination.

In several fuel meltdown experiments, aerosol particle sizes, chemical identification and associated radioactivity were determined and size comparisons were made by electron microscopy. The ease of particle measurement by this device has contributed an extra benefit in terms both of the characterization of chemical forms of airborne radioactivity as well as to a simple model of aerosol formation and agglomeration.

---

*Research sponsored by the U.S. Atomic Energy Commission under contract with the Union Carbide Corporation.

[/]Present address: Hahn-Meitner Institut Für Kernforschung, Berlin, Germany.

1. INTRODUCTION

Particles having a diameter of about 0.1 μ and less are highly retained in the respiratory tract,[1] and particles in this size range are expected to be released as a consequence of a more or less severe core meltdown in a reactor accident.[2] Large particles are removed quickly from the atmosphere by sedimentation whereas particles having a diameter less than 1 μ remain airborne long enough to constitute a hazard. The hazard is a consequence both of their high retention in the respiratory tract and their radioactivity.

Knowledge concerning the size distribution of particles released in simulated reactor accidents and the radioactive species carried by them is still lacking because suitable instruments to measure size distribution are not available. Predictions of the conditions in a real reactor accident are therefore unreliable.

A modified cascade impactor can provide some of the needed data. This device not only separates particles having different sizes, but also permits identification of the radioactive species which each size group is carrying. Impactors are ordinarily limited to particles larger than 0.5 μ, whereas particles of 0.1 μ and smaller are of interest in nuclear safety research. The efficiency of depositing smaller particles in an impactor can be improved by operating the impactor at low pressure.[3,4]

2. THEORETICAL CONSIDERATIONS

The basic theory of the impaction principle is quite simple. When a gas jet carrying particles is directed toward a surface, all particles having sufficient inertia leave their stream lines and settle on the surface. Smaller particles remain within the jet stream. In the next stage,

the gas passes through smaller holes and the jet is accelerated to a higher velocity. The probability of smaller particles settling is thus increased. This basic principle is demonstrated in Fig. 1.

It was first found by K. R. May[5] that the efficiency for depositing particles depends on a dimensionless term, called the impaction parameter, which is characteristic for each type of impactor. Efficiency curves were then calculated by W. E. Ranz and J. B. Wong[6] and by C. N. Davies and M. Aylward[7] for circular and rectangular jets in different geometrical arrangements. A plot of the efficiency versus impaction parameter always shows the characteristic S-shape. This theoretical relation is verified by experimental results. Using the relationship between impaction parameter and particle diameter, given in Eq. (1), one can calculate the efficiency for depositing a certain particle size from the efficiency curves.

$$\psi = \frac{C\rho D^2 v}{18\eta D_j} \tag{1}$$

ψ = impaction parameter, dimensionless

C = Cunningham correction, correction for particles with sizes comparable to the mean free path of the gas molecules

ρ = specific gravity of particles, g/cc

D = diameter of particles, cm

η = viscosity of gas, poise

D_J = diameter of jet, cm

v = velocity of jet, cm/sec.

The derivation of Eq. (1) is based on the following basic assumptions: spherical particles of negligible size, viscous gas flow, uniform velocity field and no bounce of particles. The efficiencies calculated are somewhat higher than observed.

ORNL-DWG 67-3272

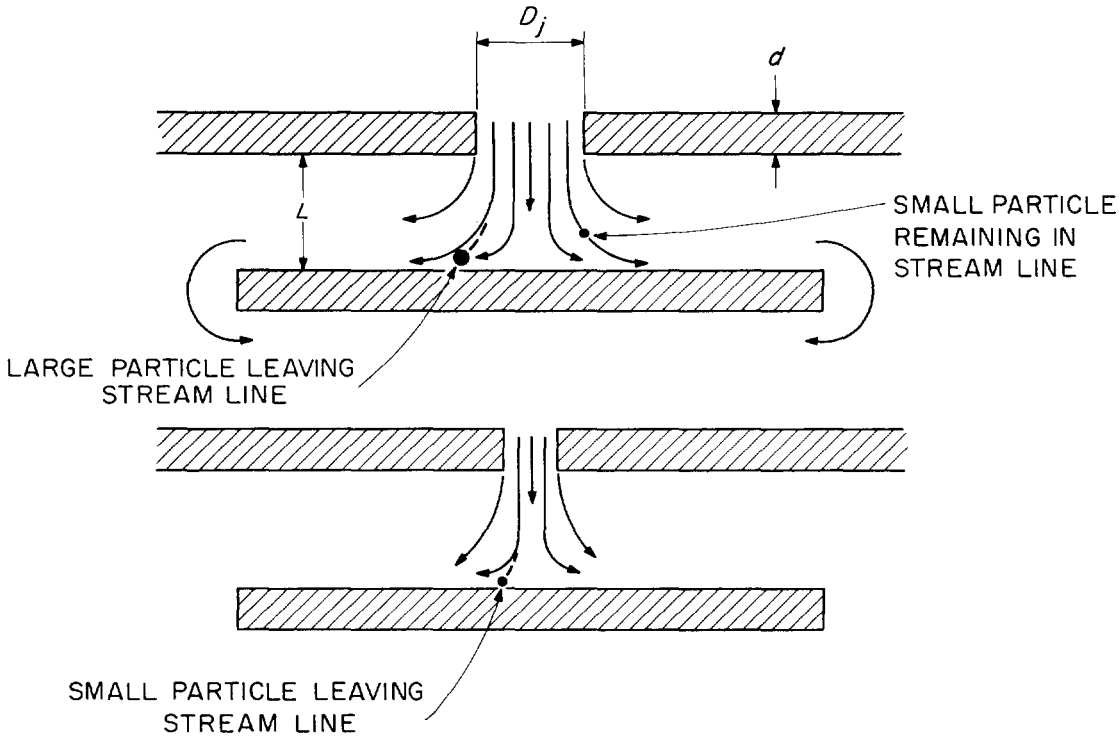

Fig. 1. Impaction Principle

If ψ approaches 1, the deposition efficiency will become 100%. On the other hand, if $\psi = 0$, the deposition efficiency is zero also. In the range between $\psi = 1$ and $\psi = 0$, the efficiency increases continuously with ψ according to an S-shape characteristic. It is quite common to compare the performance of impactor stages by the diameter of particles deposited with a 50% efficiency. This diameter shall be called D_{50} or the stage constant and the corresponding impaction parameter ψ_{50}.

In search of ways to increase the efficiency of depositing submicron particles, Eq. (1) may be examined. Because ψ is replaced by ψ_{50}, a constant of the impactor stage, the right side of the equation also becomes constant. Therefore, three factors remain to influence the value of D_{50}. These are the Cunningham-Correction describing the slip of particles in the gas stream, the jet velocity and the jet diameter. In order to lower D_{50} beyond 0.5 μ by changing v and D_j, it would be necessary to exceed 1/3 of the velocity of sound or to drill holes smaller than 0.2 mm in diameter. But these values are practical limits; particles of velocity greater than 1/3 Mach bounce significantly and the deposition is lowered by an unknown factor.[8] In addition, the gas which enters the nozzle[9] expands adiabatically within the nozzle. Holes smaller than 0.2 mm are not only difficult to drill, especially the large number necessary to maintain the gas flow, but they also have the disadvantage of imposing significant pressure drops.

The applicability of the impaction theory at reduced pressure was verified by S. C. Stern et al.[10] taking into account the pressure dependence of the Cunningham-Correction in Eq. (1). Another proof was given by A. F. McFarland and H. W. Zeller,[8] in their experimental results of the ". . . Impactor for High Altitude." These findings indicate that the cascade impactor can be used to separate particles in the small size range of interest.

The Cunningham-Correction C, based on the work of R. A. Millikan[11] is defined according to Eq. (2).[8,10]

$$C = 1 + \frac{2\lambda}{D}\left(1.23 + 0.41\, e^{-0.44\, D/\lambda}\right) \qquad (2)$$

where λ is the mean free path of the gas molecules which constitute the gas phase and D is the diameter of the particles. In air:

$$C = 1 + \frac{10^{-2}}{pD}\left(1.23 + 0.41\, e^{-86pD}\right) , \qquad (2a)$$

where p is the air pressure (mm Hg) and the particle diameter, D, is in cm. C increases, if the mean free path of the gas molecules increases. C is larger for smaller particles. At atmospheric pressure, C is about equal to unity for particles larger than 1 μ (see Fig. 2). By decreasing the pressure, C can be readily increased by more than two orders of magnitude for the particle sizes of interest. D_{50} is decreased by more than one order of magnitude, because (C) x (D_{50}^2) is constant according to Eq. (1).

The correction Millikan applied was relatively small, because λ/D was smaller than 47, whereas in the device reported by McFarland and Zeller[8] reasonable results were also obtained for $\lambda/D = 1000$, which means that C was about 6000. Thus, the application of Eq. (2) is justified for high correction values, too. In the experiments reported here, C was always less than 1000.

The jet velocity at the nozzle outlet may be replaced by the gas flow Q into the nozzle, a function of the nozzle diameter $\pi/4\ D_j^2$ and the ratio of gas density at the inlet and outlet, ρ/ρ_o.

$$v = \frac{Q}{\frac{\pi}{4} D_j^2\ \rho/\rho_o} . \qquad (3)$$

If Q is replaced by the external gas flow Q_a, the ratio of external to internal pressure pa/p and the number of nozzles N, Eq. (3) becomes,

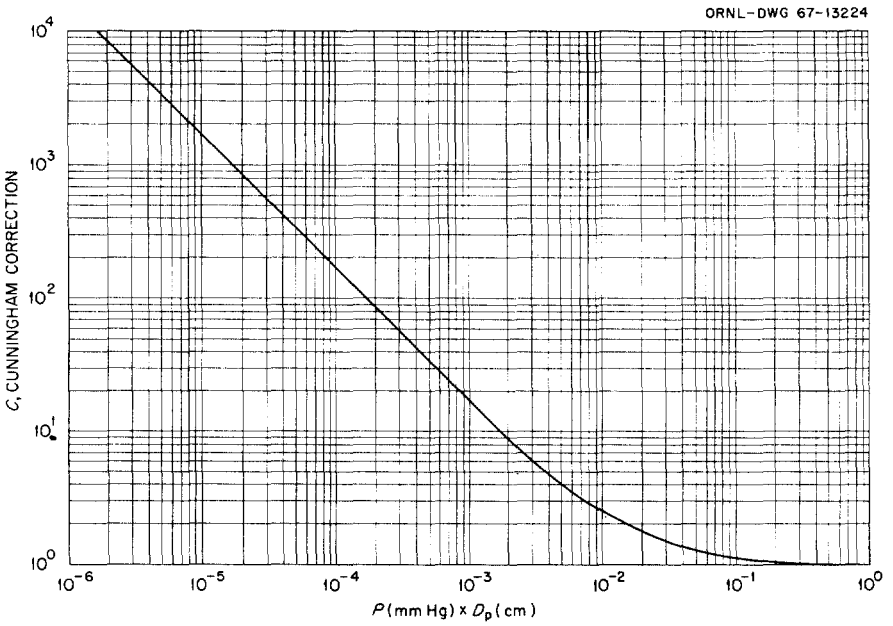

Fig. 2. Cunningham-Correction vs Pressure Times Particle Diameter.

$$v = \frac{p_a Q_a}{p \frac{\pi}{4} D_j^2 N \rho/\rho_o} \quad . \tag{4}$$

Denoting $p\ (\rho/\rho_o) = p_o$, inserting (4) into (1) one obtains

$$\psi_{50} = \frac{C(p_o, D_{50})\rho\ p_a Q_a\ D_{50}^2}{18\eta\ D_j^3 p_o \frac{\pi}{4} N} \quad . \tag{5}$$

If p_o(mm Hg) x D_{50} (cm) $< 10^{-3}$, C is approximately,

$$C \cong 3.3 \frac{\lambda}{D_{50}} \cong \frac{1.7 \times 10^{-2}}{p(\text{mm Hg}) D_{50}(\text{cm})} \quad ,$$

and (5) becomes

$$\psi_{50} = \frac{1.7 \times 10^{-2}\ \rho p_a Q_a\ D_{50}}{18\eta\ D_j^3\ p_o^2 \frac{\pi}{4} N} \quad . \tag{6}$$

Assuming a constant jet velocity, Eq. (4) and Eq. (6) may be combined to obtain

$$D_{50} \sim p_o D_j$$

and $Q_a \sim D_{50}\ D_j\ N$.

These are fundamental relationships in low pressure impactor operation. D_{50} depends only on the internal pressure and nozzle size, whereas the external gas flow depends on the number of nozzles too. It is easier to obtain a small D_{50} value at low gas flow than at high gas flow. Small D_{50} at a high flow rate can be achieved only with a great number of nozzles.

The slip effect which on the one hand enables the impaction of small particles; on the other hand, reduces acceleration of the particles to the jet velocity. Particles not at jet velocity would have a smaller deposition

efficiency. An estimate of the slip in velocity is easily obtained from the basic equations of the impaction theory.[6,8]

The motion of particles in a nozzle of constant diameter can be described by equating the force of inertia of the particle to the force of viscous drag by the medium as shown in Eq. (7),

$$m\dot{v}_p = \frac{3\pi\eta\, D_p}{C} (v_p - v_j) \quad , \tag{7}$$

where v_p is the component of velocity of particles in the direction of the jet, v_j is the jet velocity (parallel to the nozzle axis), m is the particle mass and is equal to $\rho \frac{\pi}{6} D_p^3$, D_p is the particle diameter.

$$\text{On taking} \quad \dot{v}_p = \frac{dv_p}{dx} \cdot \frac{dx}{dt} = \frac{dv_p}{dx} v_p \quad .$$

Substituting and rearranging, one obtains

$$\frac{dv_p}{dx} = - \frac{18\eta}{\rho C D_p^2} \left(1 - \frac{v_j}{v_p}\right) \tag{8}$$

and if v_j is assumed to be constant, then

$$\frac{v_p}{v_j} + \ell n \left(1 - \frac{v_p}{v_j}\right) = \left[- \frac{18\eta}{\rho C D_p^2} \frac{x}{v_j} \right]_0^L \quad . \tag{9}$$

At the limiting values of x, the following are true;

at $x = 0$, $v_p \cong 0$

at $x = L$, $v_p \neq 0$.

Applying Eq. (1) it follows that,

$$\frac{v_p}{v_j} + \ell n \left(1 - \frac{v_p}{v_j}\right) = - \frac{L}{\psi D_j} \quad . \tag{10}$$

This equation is plotted in Fig. 3. Beyond $L/(\psi D_j) = 10$ the slip in velocity is negligible. In practice, the region in which v_j is considered to be constant should be twice as large as the diameter.

The size distribution of the aerosol is obtained from the amounts of deposited material on the stages and the stage constants. T. T. Mercer[12] prefers the use of the effective cut-off diameter, ECD, rather than the mass median diameter, MMD, as the stage constants, because with the latter one depends much more on the aerosol size distribution than with the ECD. In the ECD approximation the efficiency curve is approximated by a step function. Below ECD the collection efficiency is presumed to be zero and above ECD the efficiency is unity. In this approximation the actual amount of material collected below ECD is compensated by the amount lost above ECD. The following shows how the size distribution of the aerosol can be evaluated in the ECD approximation if the relative amount of material on the impaction stages is known. N_i is the amount of material on stage i, $\eta_i(D)$ is the efficiency of deposition of particles of diameter D. $n(D) \times dD$ is the number of particles in the size range D ... D + dD.

$$N_1 = \int_{D=0}^{D=\infty} n(D)\ \eta_1(D)\ dD = \int_{ECD_1}^{\infty} n(D)\ dD \tag{11}$$

$$N_2 = \int_0^{\infty} n(D)\ \eta_2(D)\ [(1 - \eta_1(D)]\ dD =$$

$$\int_0^{\infty} n(D)\ \eta_2(D)\ dD - \int_0^{\infty} n(D)\ \eta_1(D)\ \eta_2(D)\ dD =$$

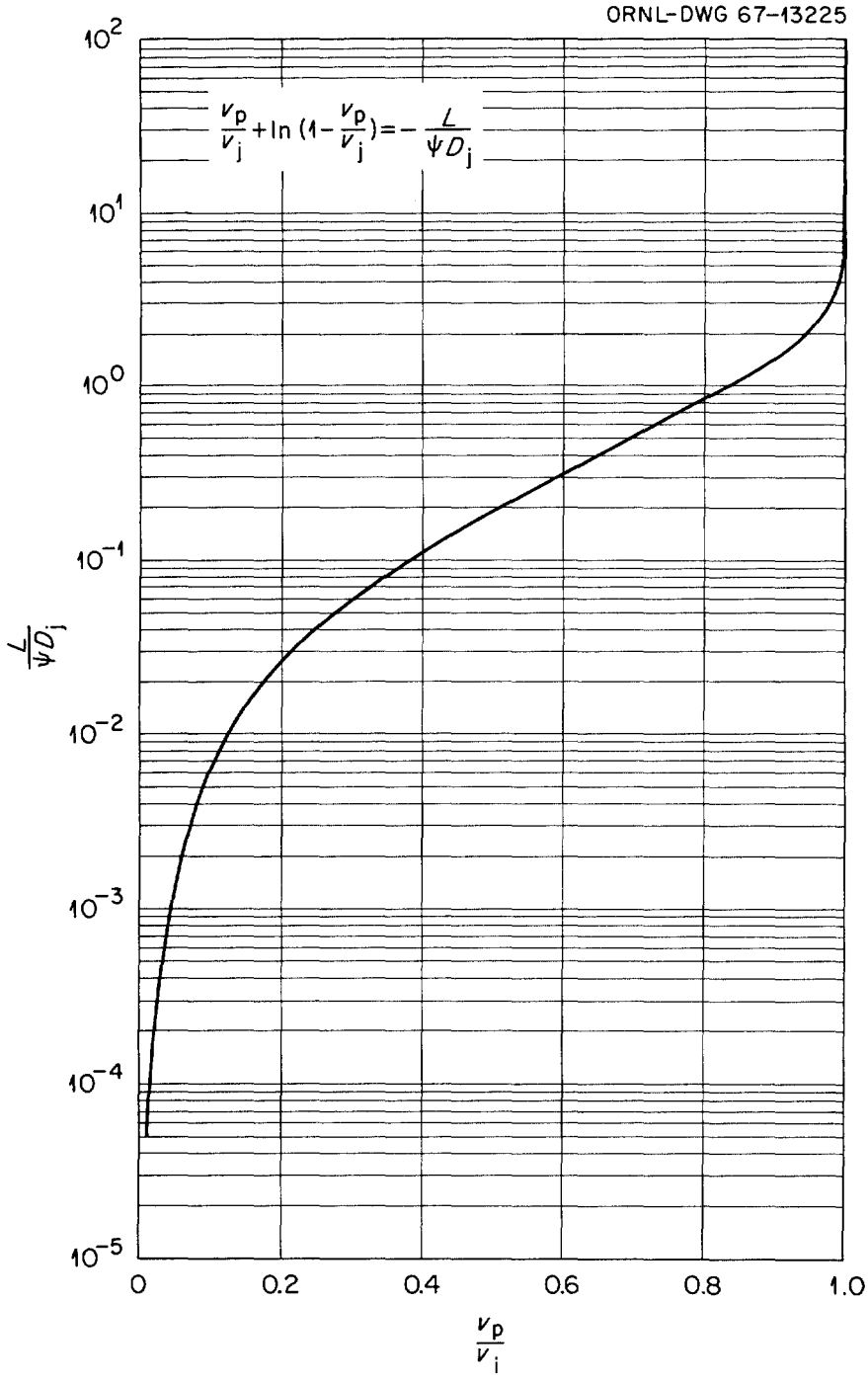

Fig. 3. The Dependence of Relative Particle Velocity on Impaction Parameter.

$$\int_{ECD_2}^{\infty} n(D)\, dD - \int_{ECD_1}^{\infty} n(D)\, dD = \int_{ECD_2}^{ECD_1} n(D)\, dD \quad . \tag{11a}$$

$$N_i = \int_{ECD_i}^{ECD_{i-1}} n(D)\, dD \quad . \tag{11b}$$

Assuming infinitesimal steps, the size distribution is obtained:

$$n(D) = \frac{N_1}{ECD_{i-1} - ECD_i} \quad . \tag{12}$$

It is easy to see from Eq. (11) that ECD depends on the aerosol size distribution. Therefore in practice the ECD_i are usually not known and the smoothness (and hence the accuracy) of the frequency distribution [n(D)] is limited by the number of impactor stages. In a reasonable approximation, ECD is replaced by the stage constants (D_{50}) which is only a characteristic constant of the impaction stage and does not depend on the aerosol size distribution. The closer the efficiency curve approaches a step function the more accurate this approximation becomes.

3. EXPERIMENTAL APPROACH

3.1 General Assembly

The general assembly used in most cases is shown schematically in Fig. 4, and a photograph of the assembly is given in Fig. 5. Air is drawn by suction through the furnace (in which particles are formed by vaporization and condensation in the cool air stream) and through valve V-2. A dryer unit D and a charcoal cartridge F reduces humidity and the concentration of natural aerosol. The air flow is

ORNL-DWG 67-3274R

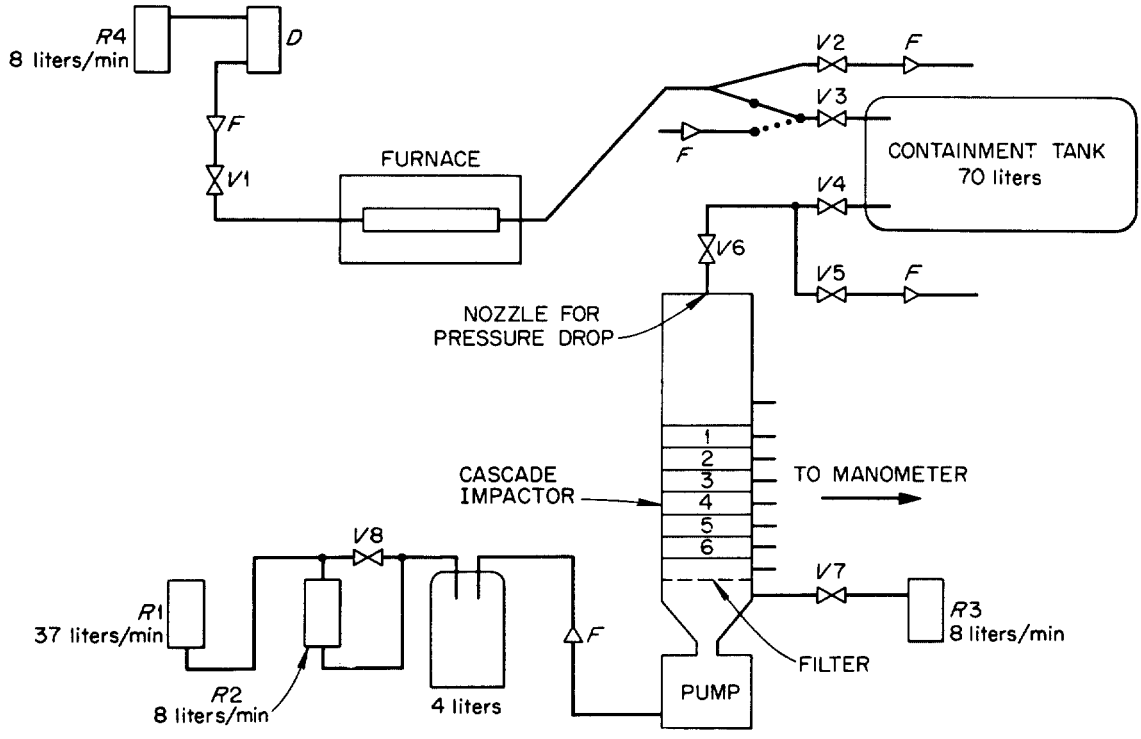

Fig. 4. Schematic Flow Diagram.

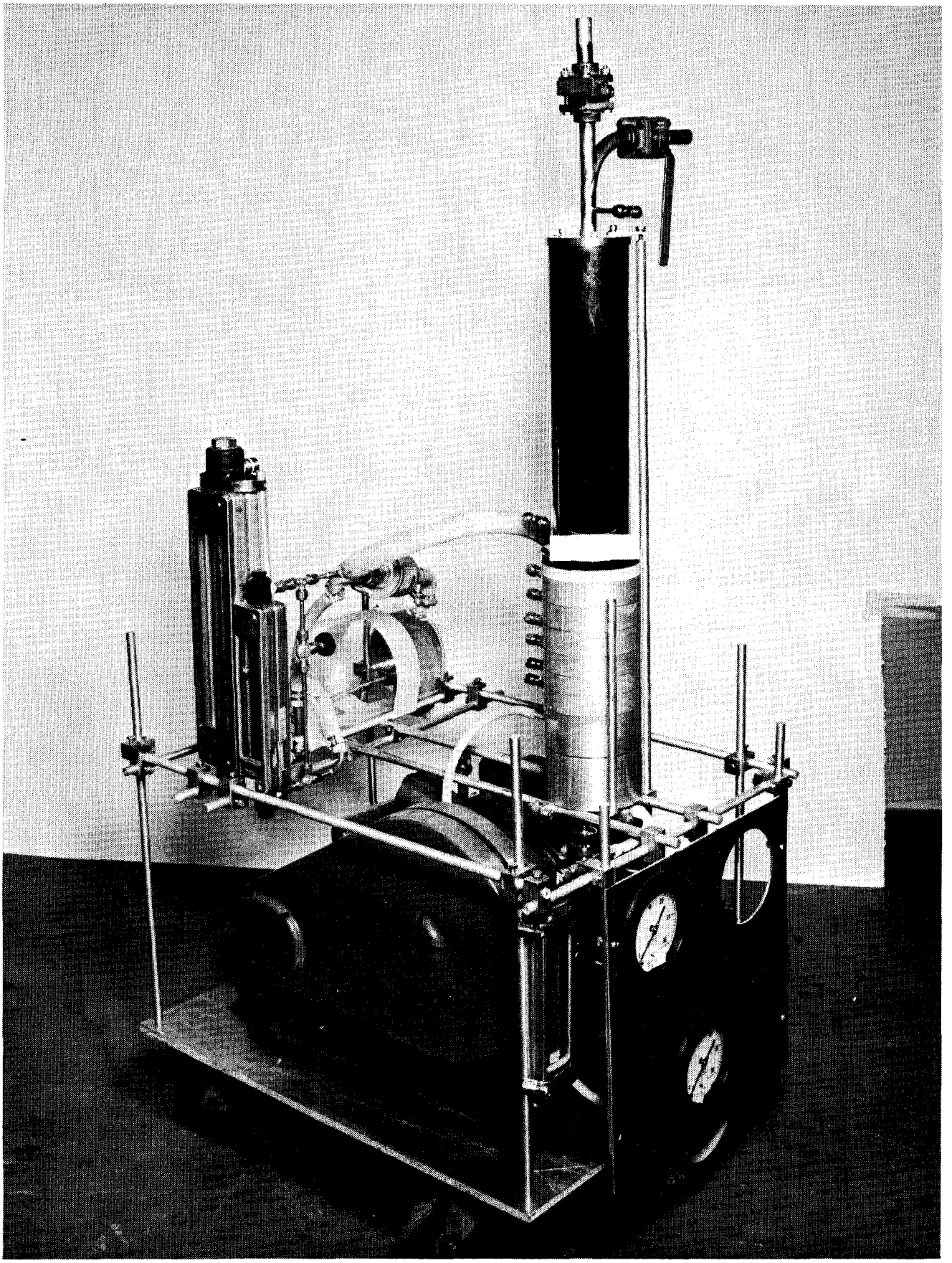

Figure 5 Impactor Assembly

controlled by valve V-1 and indicated by the flow meter R-4. After steady state conditions for the furnace temperature are established, the by-pass to the 70-liter containment tank (V-2) is closed and the containment tank is filled with the particles by suction through valve V-5. Filter samples taken upstream of V-2 enable one to check the approach of a steady-state particle generation rate.

The particles are enclosed in the containment tank for a certain time (about 1 hr). During this aging period, the mass median diameter increases by agglomeration until the right size for the sampler is reached. Before the particles are directed into the sampler, steady flow conditions in the sampler are established by suction of the pump below the sampler and flow through an open by-pass line, V-5. The particles are directed to the sampler, by closing valve V-5 and opening V-4. At the same time the flow from the furnace to the containment tank is replaced by a supply of cleaned air.

The low pressure in the sampler is generated by a pressure drop at a flow nozzle and by the amount of air added through valve V-7. If desired, the air flow through the sampler can be changed by another nozzle size. The first stage of the sampler is positioned in a distance far enough from the nozzle (about 5 times the sampler diameter) so that it can be assumed that the spread of the jet is sufficient to cover the whole diameter of the first stage. All particulate matter penetrating the stages are held up in a back-up filter. Provisions are made to measure the pressure at several points in the sampler as indicated. Additional flow controls are provided by flow meters R-1, R-2, and R-3. A closer look at the arrangement of the flow nozzle, impactor stages and back-up filter is presented in Fig. 6.

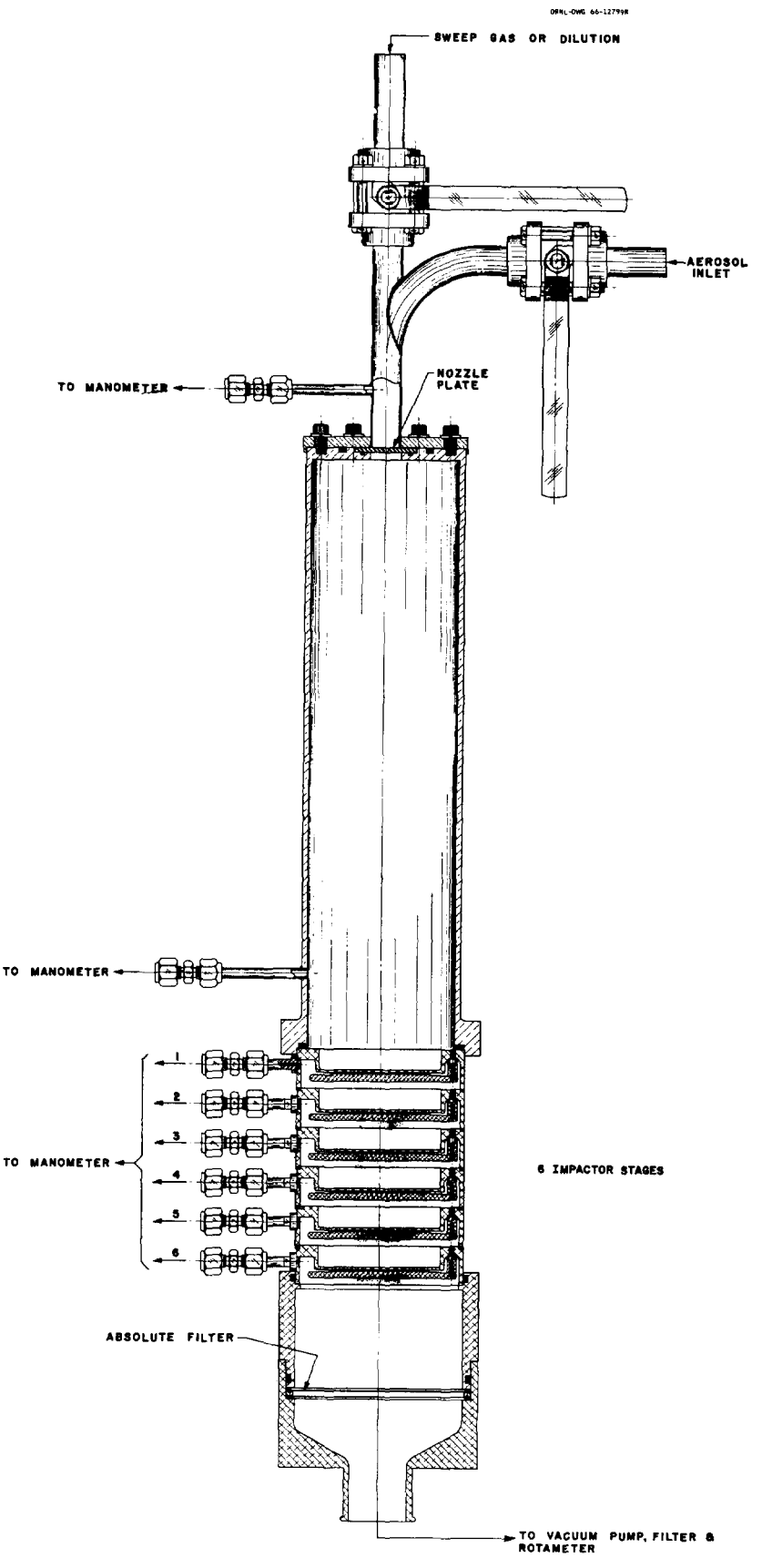

Fig. 6. Low-Pressure Cascade Impactor Mark-I.

The first direct application in nuclear safety research was during a CRI run, in which the behavior of released fission products was the main interest. Two gas samples were taken and analyzed with the Low-Pressure Cascade Impactor. A description of the Containment Research Installation (CRI) and the release of simulated fission products is reported elsewhere.[13] More experimental details will be given in Section 3.6.

3.2 Particle Generation

In the cases in which only the function of the low-pressure cascade impactor was tested and a variable supply of aerosol was acceptable, material was vaporized from an open boat and condensed in a cool air stream. The boat was inserted into a tube heated by an electric furnace (see Fig. 4). By this technique, particles from nichrome wire, PbI_2, NaCl and $CsNO_3$ were generated.

In order to prove the uniformity of deposition, the black painted impaction plates were heavily loaded with white NaCl particles. The size distribution was not wide enough to cover all 6 stages, therefore only the last 4 stages show particle deposition in Fig. 7. The sizes of the spots are not as equal as they should be, indicating slight differences in deposition efficiency between the jets.

As described in ORNL-4226,[14] the stage constants* of the Andersen Sampler under low pressure were obtained by an experimental method. Calculated and measured stage constants* do not agree in the first stages but become quite comparable for stages 4 to 6. Some reasons for this behavior are discussed in the Appendix.[14] Based upon the calibration, the stage constants for each stage were calculated for several specific

*Particle diameter cutoff point or D_{50} in Eq. (6).

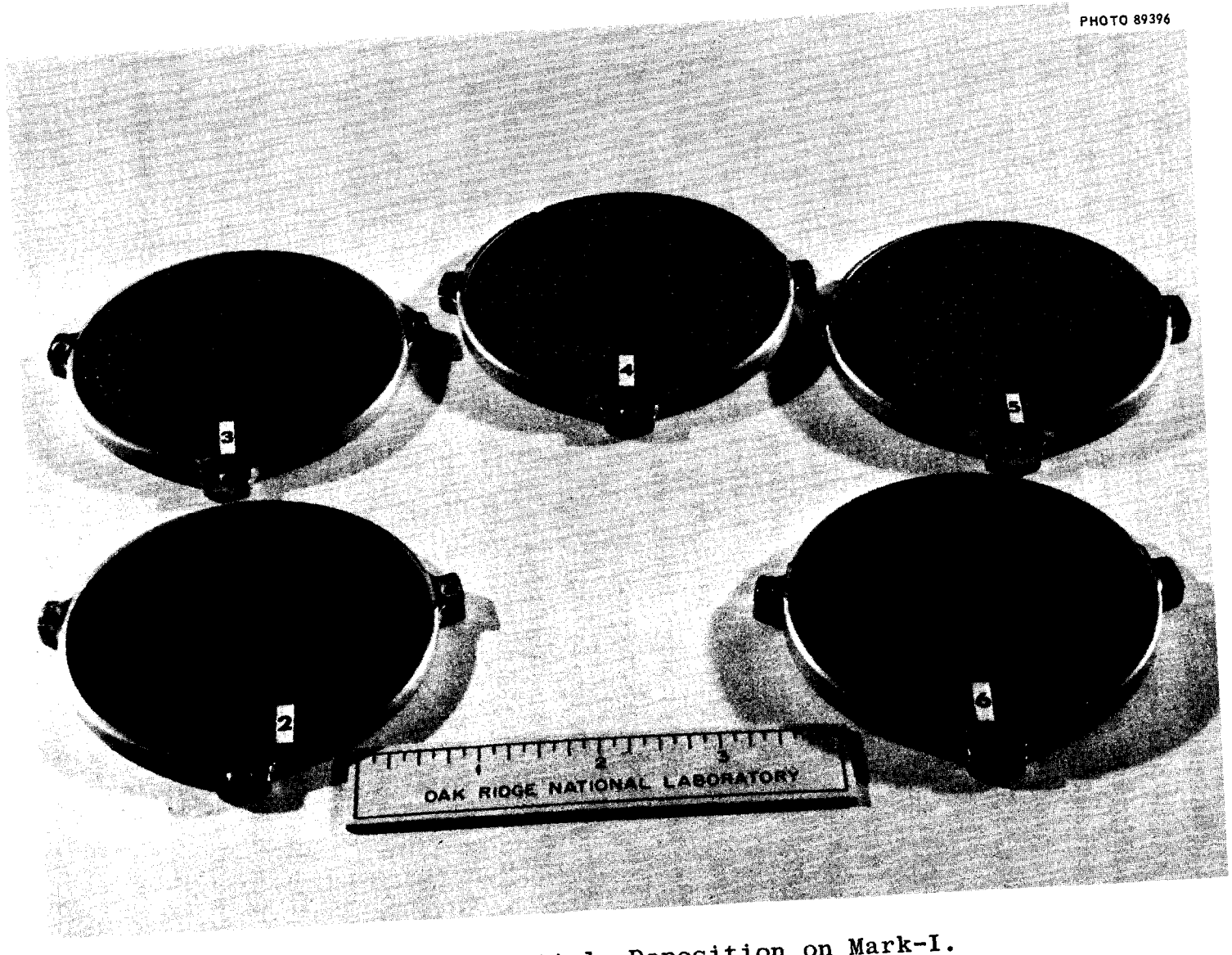

Fig. 7. Particle Deposition on Mark-I.

gravities of particles using Eq. (6). The pressure at each stage was taken at an air flow rate of 8 liters/min. Figure 8 graphically shows the results.

Some experiments were performed at the University of Minnesota with spherical particles of known size and a very narrow size distribution, in order to calibrate the low-pressure cascade impactor. These particles were produced either in a atomizer-impactor combination from a uranine dye solution or in a spinning disk generator from a uranine dye solution with methylene blue added, as described by K. T. Whitby et al.[15]

3.3 Low-Pressure Cascade Impactor Mark I

The first tests were performed with the Andersen Sampler 0101,[16] the deposition efficiency of which has been measured, for instance, by J. C. Couchman.[17] The stage constants were calculated as a function of pressure using Eq. (6) and assuming that the reported impaction parameter, $\psi_{50} = 0.2$, is unchanged under low pressure operation. The results are shown in Fig. 9 in which the stage constants are plotted versus the stage number for different pressures and specific gravity of particles. Decreasing pressure and increasing specific gravity will lower the stage constants in all stages. At about 40 mm Hg the sampler covers just the size range of interest. On this basis the work was started with the Andersen Sampler 0101 after some modifications were done (the modified Andersen Sampler is called Mark-I).

3.4 Low-Pressure Cascade Impactor Mark-II

Besides the modified Andersen Sampler (Mark-I), our own design (Mark-II) was built. This model was specially designed for low pressure operation, small pressure drop, easy decontamination and quick exchange of sample plates. Again,

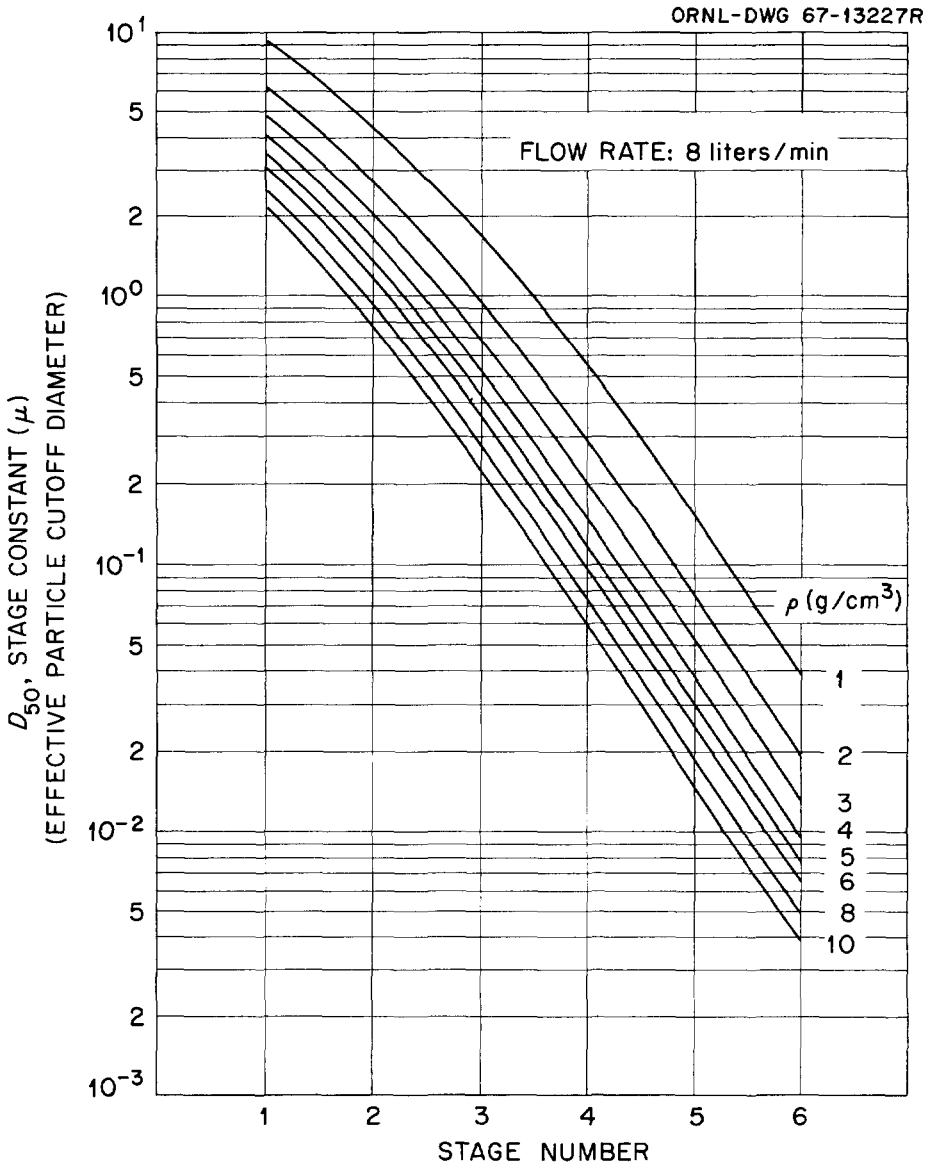

Fig. 8. Calculated Calibration of Mark I Impactor.

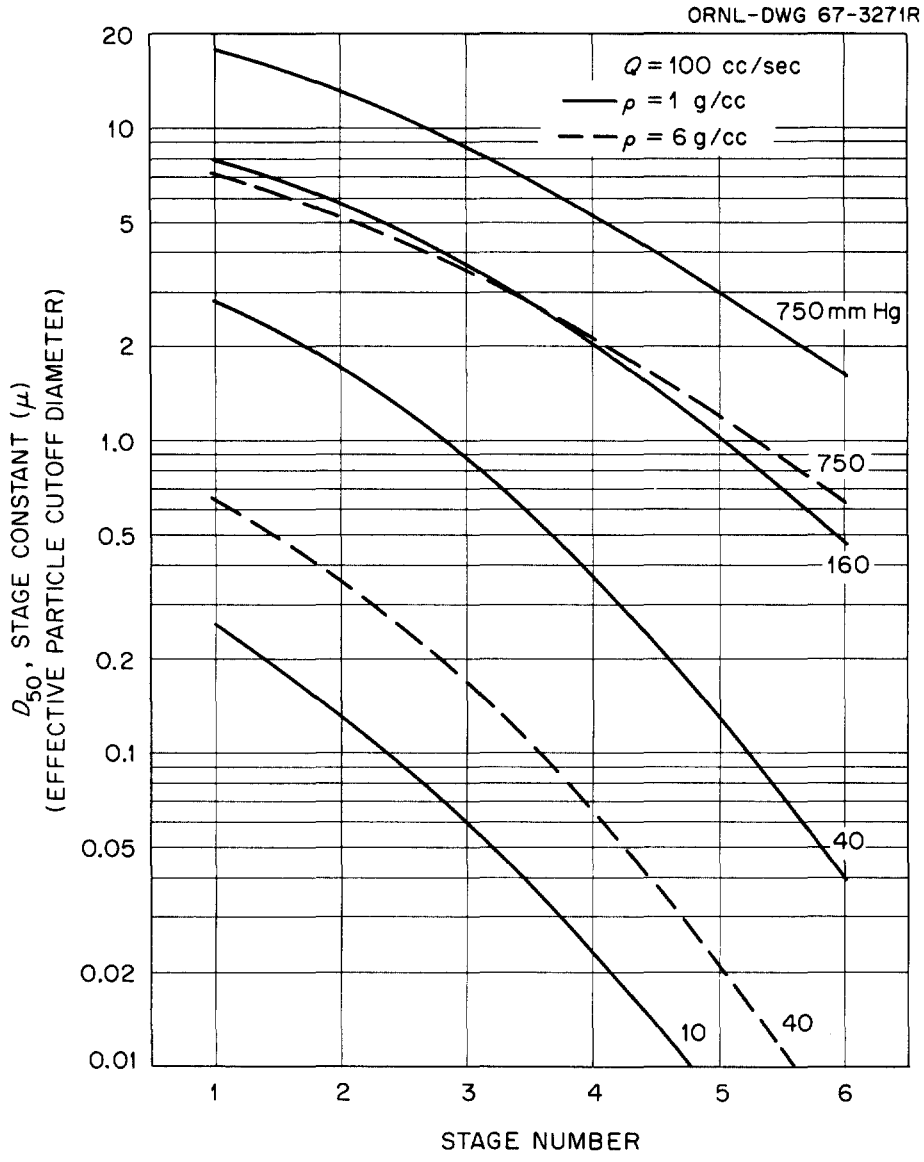

Fig. 9. Calculated Stage Constant Dependence of Andersen Sampler on Pressure and Specific Gravity of Particles.

as for the Andersen Sampler, the sample plates were designed for easy fabrication so that they could be discarded after one use and reduce the efforts required for decontamination. Hole diameter and number of holes were calculated to provide a desirable increase in D_{50} of a factor of three from stage to stage for particles of specific density 6 g/cc. The impaction parameter was assumed to be 0.15 in this calculation. Smaller clearances between sample plates and hole plates were used than in the modified Andersen Sampler to improve the particle size separation, i.e., to make sharper separations. Design data are shown in Table 1. Details of the design may be taken from Figs. 10 and 11.

Sealing between the stages is provided by O-rings. Spring loaded pins press the sample plates against three points of the support. This allows the sampler to be operated in any orientation. Tubes are connected to the stages to allow pressure measurements. At the standard air flow of 8 liters/min, the pressure drops listed in Table 2 were observed. A photograph of the stages is shown in Fig. 12. The white spots represent deposition of NaCl particles.

It was found in the test, described in ORNL-4226 that the calculated stage constants* and the experimental (Fig. 3) ones are practically identical for all stages, showing that the chosen impaction parameter ($\psi_{50} = 0.15$) was just the right one. With this verified value, stage constants for a greater variety of specific gravity of particles were calculated. The results of the calculations are plotted versus the stage number in Fig. 14. As in Fig. 11, these stage constants are to be expected only at an air flow rate of 8 liters/min and at the corresponding pressures at each stage.

The uniformity of the deposition was checked (as it was for Mark-I) with a heavy load of solid NaCl particles on the black painted impaction plates. Depositions of particles

---

*Particle diameter cutoff point of D_{50} in Eq. (6).

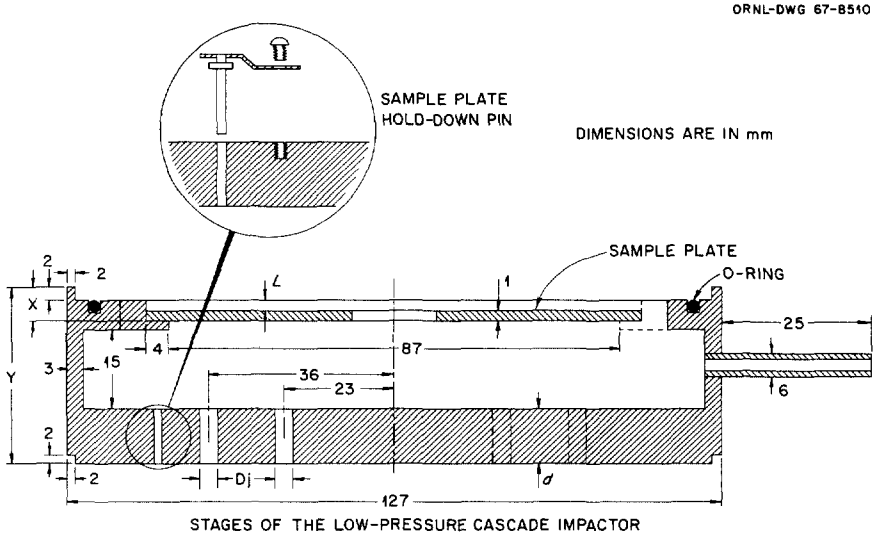

Fig. 10. Design of Mark-II (Section).

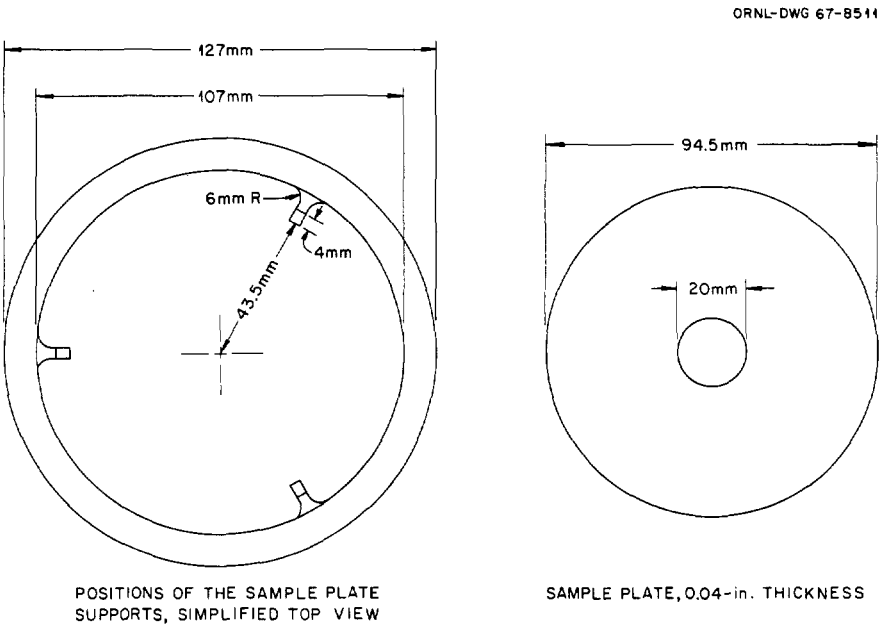

Fig. 11. Design of Mark-II (Plan).

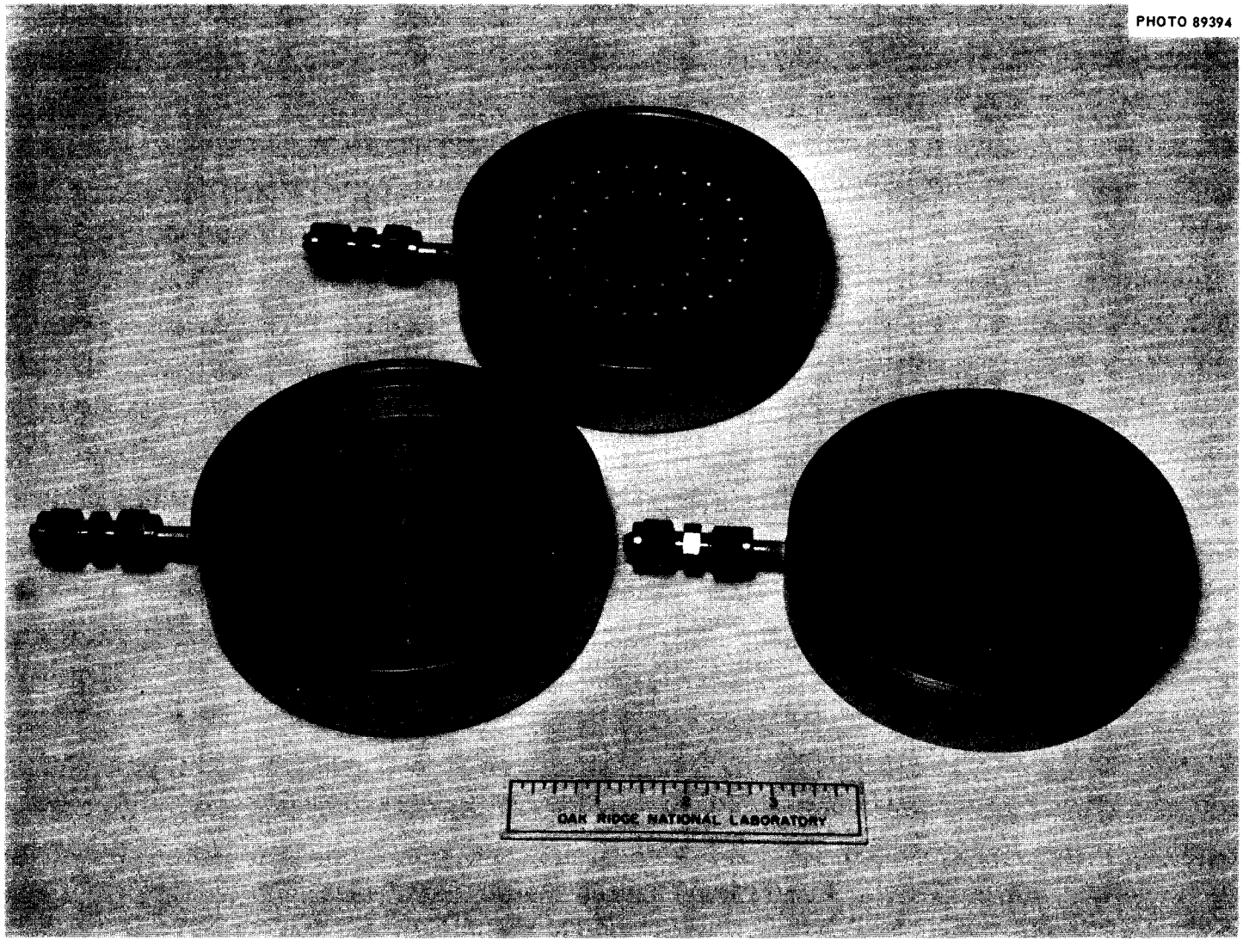

Fig. 12. Low-Pressure Cascade Impactor Mark-II.

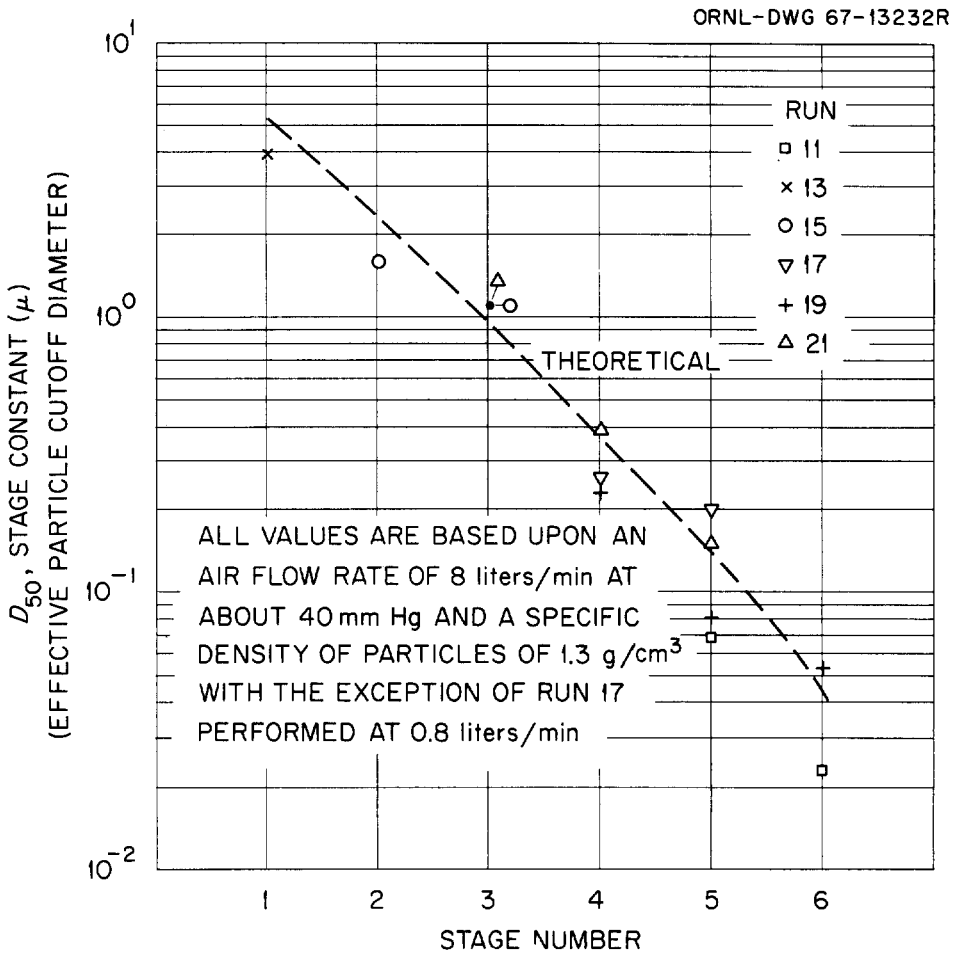

Fig. 13. Calibration of Mark-II Impactor.

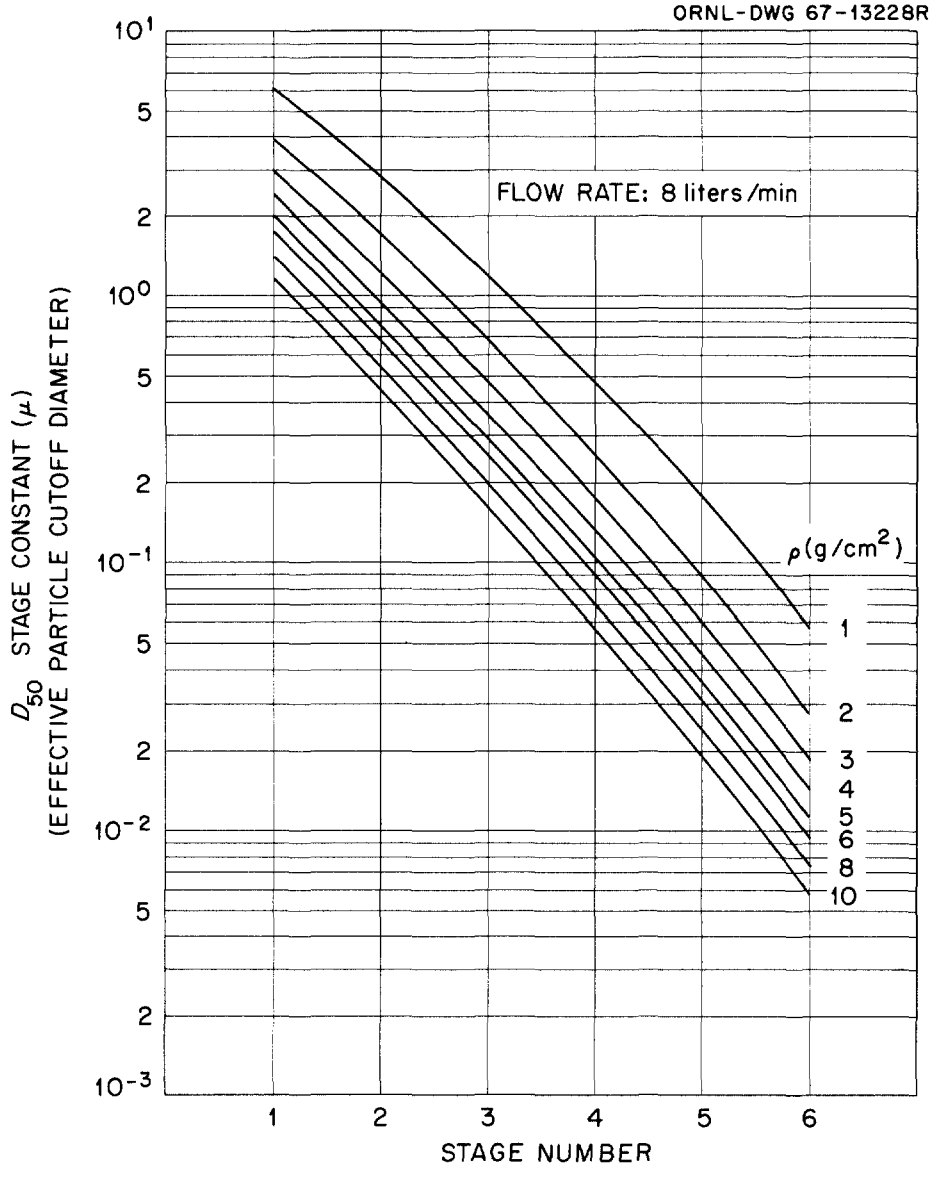

Fig. 14. Calculated Calibration of Mark II Impactor.

Table 1. Design Data for Sampler Mark-II

Stage No.	D_J(cm)	L**(cm)	N	x*(cm)	y*(cm)	d*(cm)
1	0.56	0.20	20	0.50	3.3	1.0
2	0.386	0.14	20	0.44	3.3	1.0
3	0.257	0.14	20	0.44	3.3	1.0
4	0.15	0.10	38	0.40	2.8	0.5
5	0.10	0.05	51	0.35	2.7	0.4
6	0.071	0.05	49	0.35	2.7	0.4

*Symbols refer to dimensions shown in Fig. 10.

**Denotes clearance between sample plate and hole plate.

Table 2. Pressure Drops (mm Hg)

ΔP_{1-6}*	ΔP_4	ΔP_5	ΔP_6	P_6**
19.5	0.9	3.1	14	22.7

*ΔP_i, pressure drop at stage i.

**P_6, pressure at sample plate 6.

were found on all 6 stages (see Fig. 15), and the particle spots on each stage are nearly equal in intensity. The particle size distribution was the same in both experiments, thus Figs. 7 and 15 are comparable. It is apparent that deposition was more uniform and that more stages cover the same particle size range in Mark-II (Fig. 15) than in Mark-I (Fig. 7).

3.5 Method of Analysis

The size distributions of the aerosols under investigation were evaluated by the material distribution among the impaction plates, the back-up filter and the stage constants.

In case of uranine particles, these particles were removed from the sample plates by dissolving in a known quantity of water. The intensity of fluorescence of the wash water was measured. It was proved that even from silicon coated surfaces, which were usually used, nearly all uranine particles were dissolved and only a negligible amount remained. By the calibrated reading on a fluorometer, the total mass of deposition could be calculated.

The other aerosols were radioactive tracered, in order to calculate their relative mass distribution among the stages from the radioactivity sampled on each impaction plate. A homogeneous mixture between tracer and bulk material was achieved by neutron activation in the case of nichrome wire (Cr-51) and $CsNO_3$ (Cs-134). Radioactive PbI_2 was produced by mixing inactive iodine solution with I-131 tracer solution before the PbI_2 was precipitated. Neutron activated NaCl (Na-24) was dissolved in water and then precipitated on the quartz wool. A homogeneous distribution of Na-24 in the total amount is therefore also established. The relative radioactivity of the deposited material was measured by γ counting.

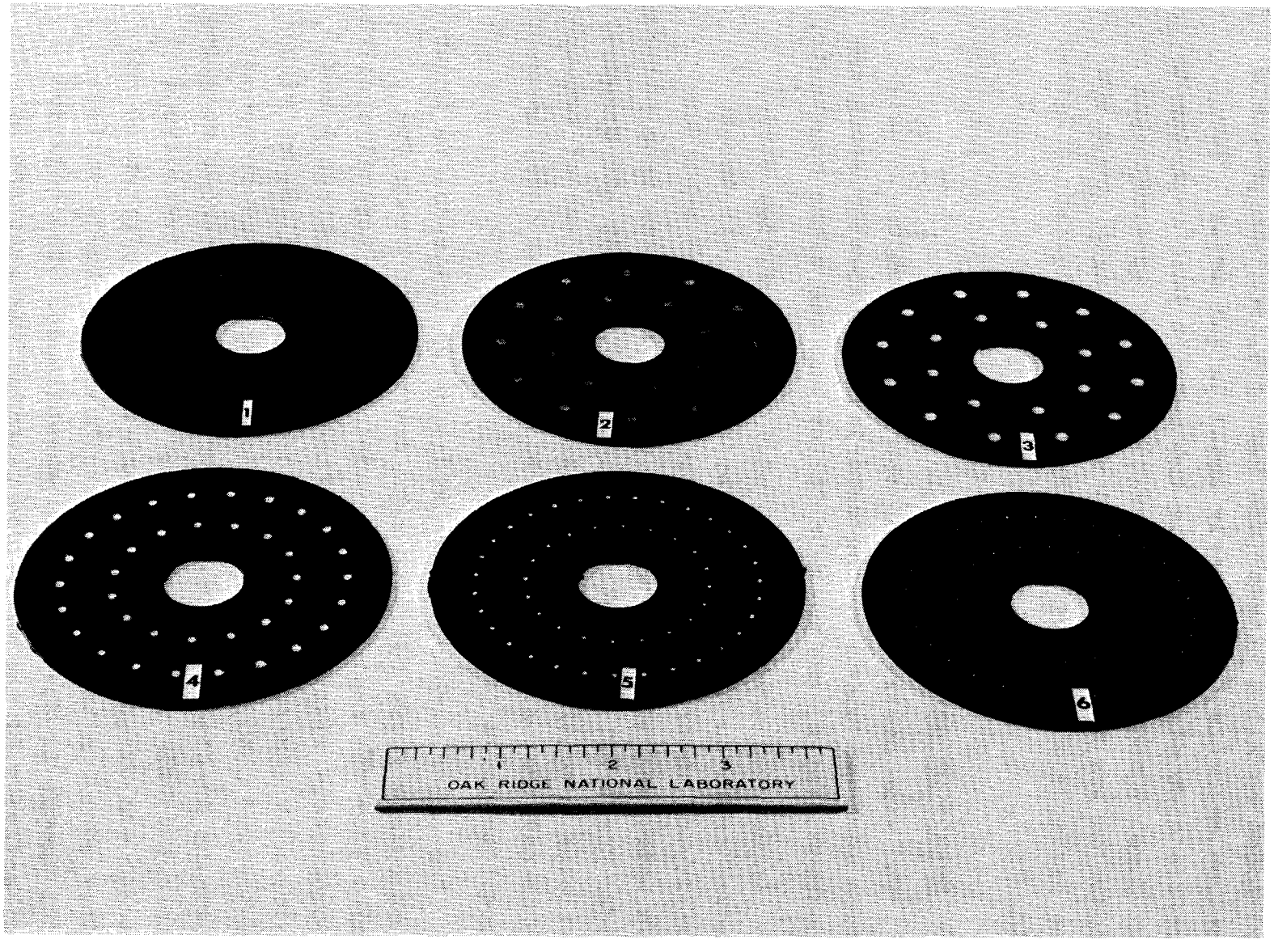

Figure 15 Particle Peposition on Mark-II

The mass of the NaCl aerosol per volume of air was checked downstream of the NaCl furnace by weighing and γ counting a Gelman GA-4 filter sample. This also provided data of the mass deposition on the sample plates by comparing the γ-count of the sample plates and the filter and from the known mass deposition on the filter (see Fig. 16).

3.6 Containment Research Installation (CRI) Experiment

The release of fission products from molten UO_2 and their behavior under reactor accident conditions was studied in run 107 in the Containment Research Installation (CRI). In order to lower the impractically high activity of a high burnup fuel element, unirradiated UO_2 was heated and the released fission products were simulated by radioactive tracered fission product elements according to a technique described by G. W. Parker et al.[13] Separately vaporized iodine, cesium, ruthenium, and tellurium passed the hot UO_2 zone in a steam atmosphere. Most of the condensation processes and particle coagulation took place in the UO_2 furnace tube and the transfer line to the reactor core. Then, entering the containment tank of the CRI the particle coagulation rate became very small because of the high dilution of their number concentration. The total amount of vaporized materials and their distribution on the components of the CRI are similar to that given below in Fig. 17 for CRI Run No. 108.

In the first Containment Research Installation test, two impactor gas samples were taken. The first gas sample of 27 liters STP was taken from the containment atmosphere between 15 and 18.5 min after meltdown and mixed with dry air in a 70-liter vessel. A second sample of 36 liters STP was transferred between 63.5 and 68 min after meltdown to the 70-liter vessel and also mixed with dry air. The vessel was swept with fresh air before the second sampling. The gas flow

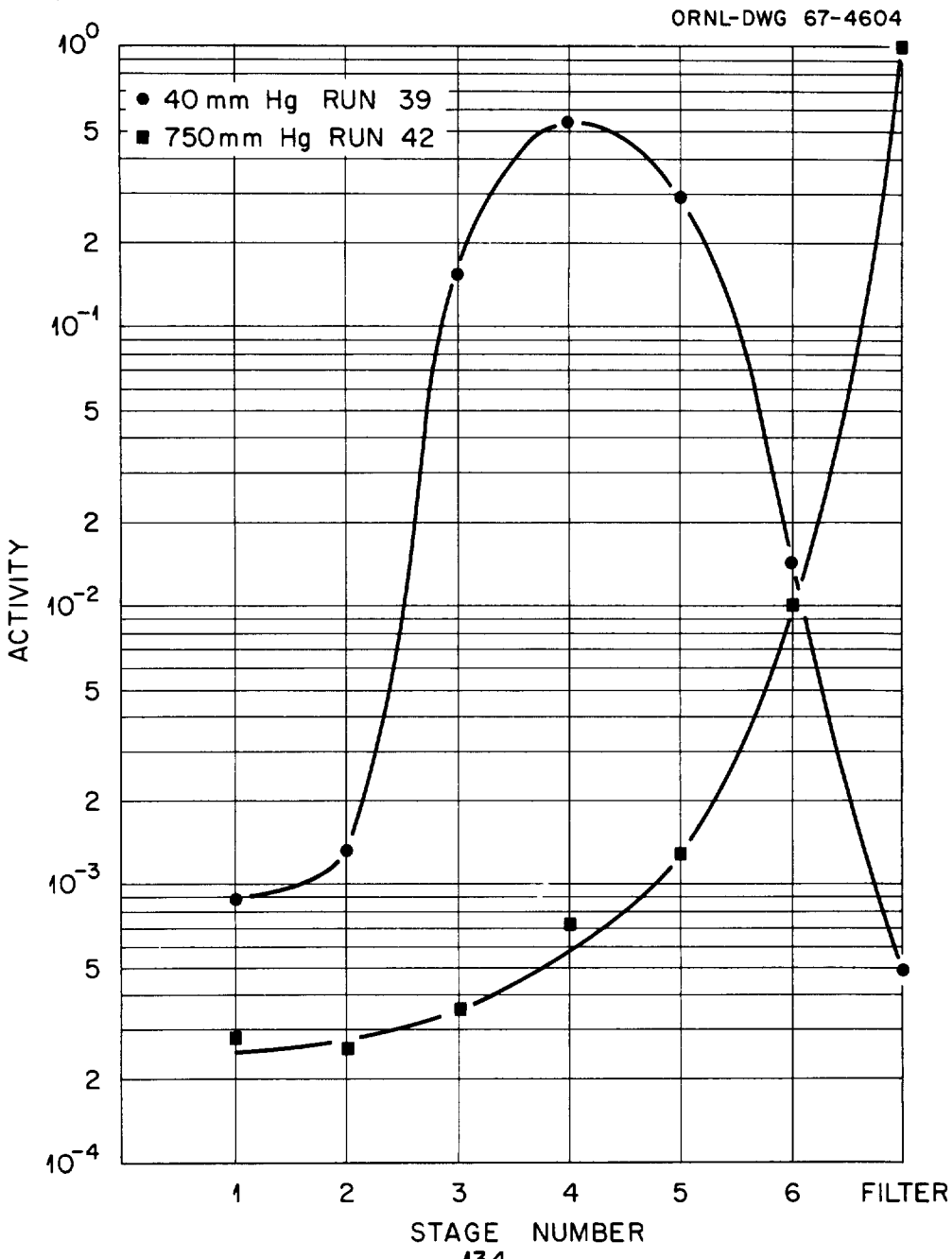

Fractional Distribution of ^{134}Cs on Stages and Filter at Different Pressures.

Fig. 16.

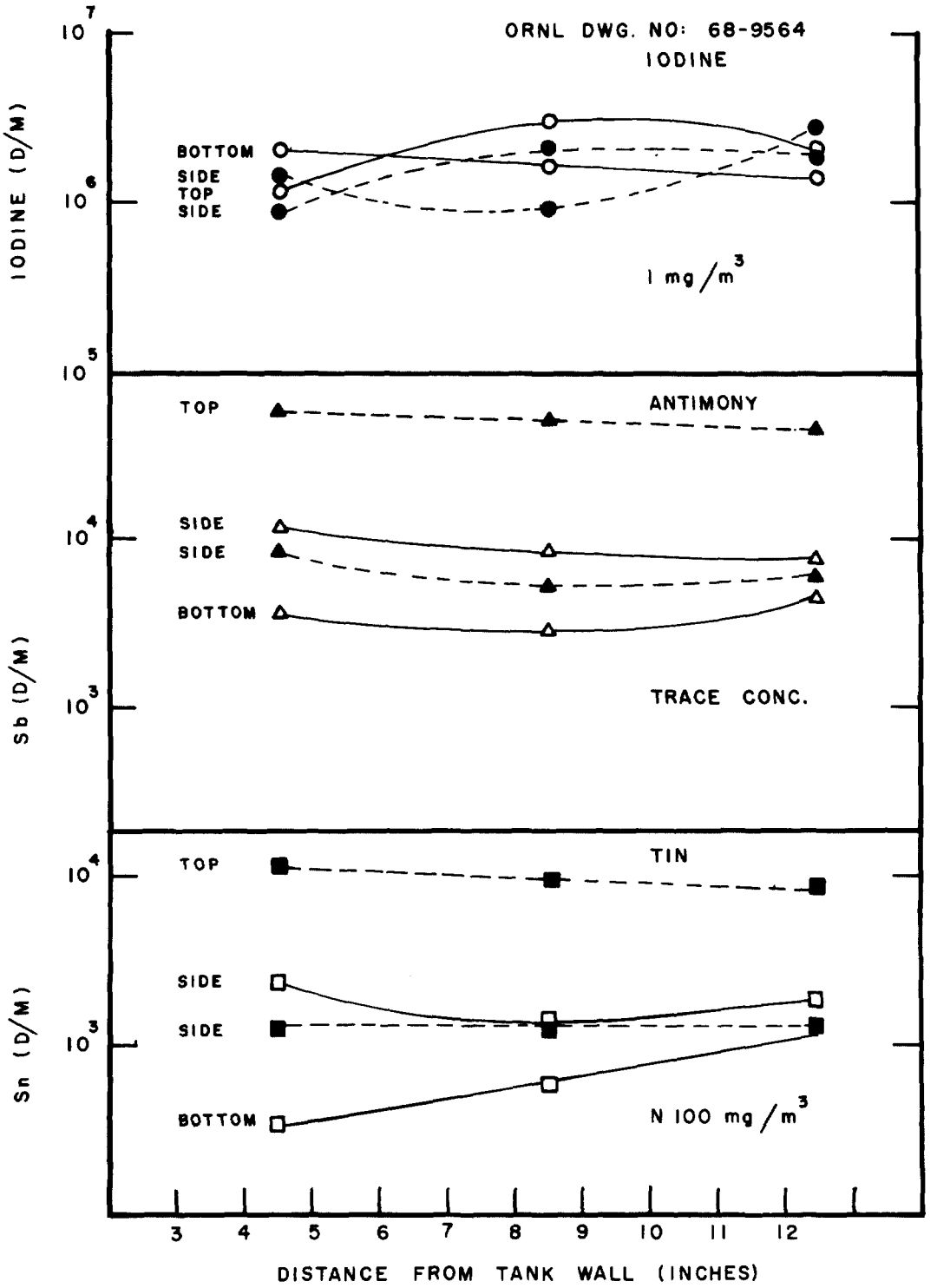

PLATE OUT ON ORIENTED COUPONS IN RUN 108

Fig. 17

rate from the CRI into the vessel was limited by an orifice or nozzle. Steam condensation in the pipe between the CRI and the sampling vessel and the flow nozzle device was eliminated by heating the walls to about 120°C.

Since the primary purpose of the cascade impactor is size classification of radioactive fission product particulates, the presence of a large amount of gaseous radioiodine could confuse the results by non-selective plateout on the sample plates. In order to minimize this effect, silver screens were used in conjunction with the impactor to reduce the fraction of gaseous iodine. The efficiency of silver screens (80 by 80 mesh silver-plated copper screen) for adsorbing gaseous iodine and the corresponding low retention for sub-micron particles was tested. In the iodine test, the iodine was produced by the bichromate method and the iodine deposition checked by the radioactivity of its tracer I-131. The penetration of NaCl particles was also measured with the screens in place.

The Low-Pressure Cascade Impactors were fitted with three silver screens in front of 5 impaction plates followed by two additional silver screens and the back-up filter. Both samplers were used in this experiment, the first gas sample was analyzed by the Mark-I and the second by the Mark-II. Fifty-eight liters (STP) of the gas contents of the vessel were passed through the sampler. All impaction plates were silicone oil coated as described previously or were covered with a membrane type organic paper. Particle loss for the screens was less than 2 percent.

3.7 Results of a Study of a Radioactive Aerosol Generated from a Zircaloy-UO_2 Fuel Meltdown

Following the initial use of the Mark-II Impactor on a "live" aerosol from Run 107, a more highly radioactive fuel sample was melted in Run 108. In this fuel specimen, the quantity of activated solids in the Zircaloy permitted

relatively accurate measurement of the concentration change in individual components (Sn, Sb, Co and Iodine) with time (Fig. 18). The Mark-II Impactor was used to test samples at two intervals, the first after 10 minutes and the second after 80 minutes. The impactor distribution analyses were identical in the two samples, one of which is shown in Fig. 19. Note that the Impactor distribution analysis for radioiodine is only slightly different from the solids which behave as if they were uniformly mixed in a single particle.

According to the deposition curve in Fig. 18, note that while the solids deposited rather uniformly without significant change in velocity, the radioiodine appeared to desorb from the solid particles and/or the tank walls and to maintain a fairly constant concentration of several percent of the starting inventory.

It was especially interesting but not surprising that the radioiodine was observed to remain susceptible to removal by chemical sprays (indicated on the iodine concentration curve in Fig. 18), although the residual particles apparently were not removed by the small amount of chemical spray used. This reversibility of radioiodine adsorption should be of considerable importance in nuclear safety hazards evaluation.

3.8 The Deposition Behavior and Size Analysis of a Fissile Material (U_3O_8) Vaporized into a Containment Vessel

Because of the relative importance in the safety of fast reactors, the vaporization and leakage of plutonium oxide has been the subject of recent studies at BNL by Castleman, et al. and by Koontz at Atomics International both for the assessment of deposition behavior as well as particle size (uranium oxide serves as a practical substitute for plutonium aerosols) and properties. In the fuel melting studies carried out in the CRI, in order to compare the effect of an increase in aerosol concentration over the range of the various accident regimes pertinent to LOFT, two cases were analyzed by means of the

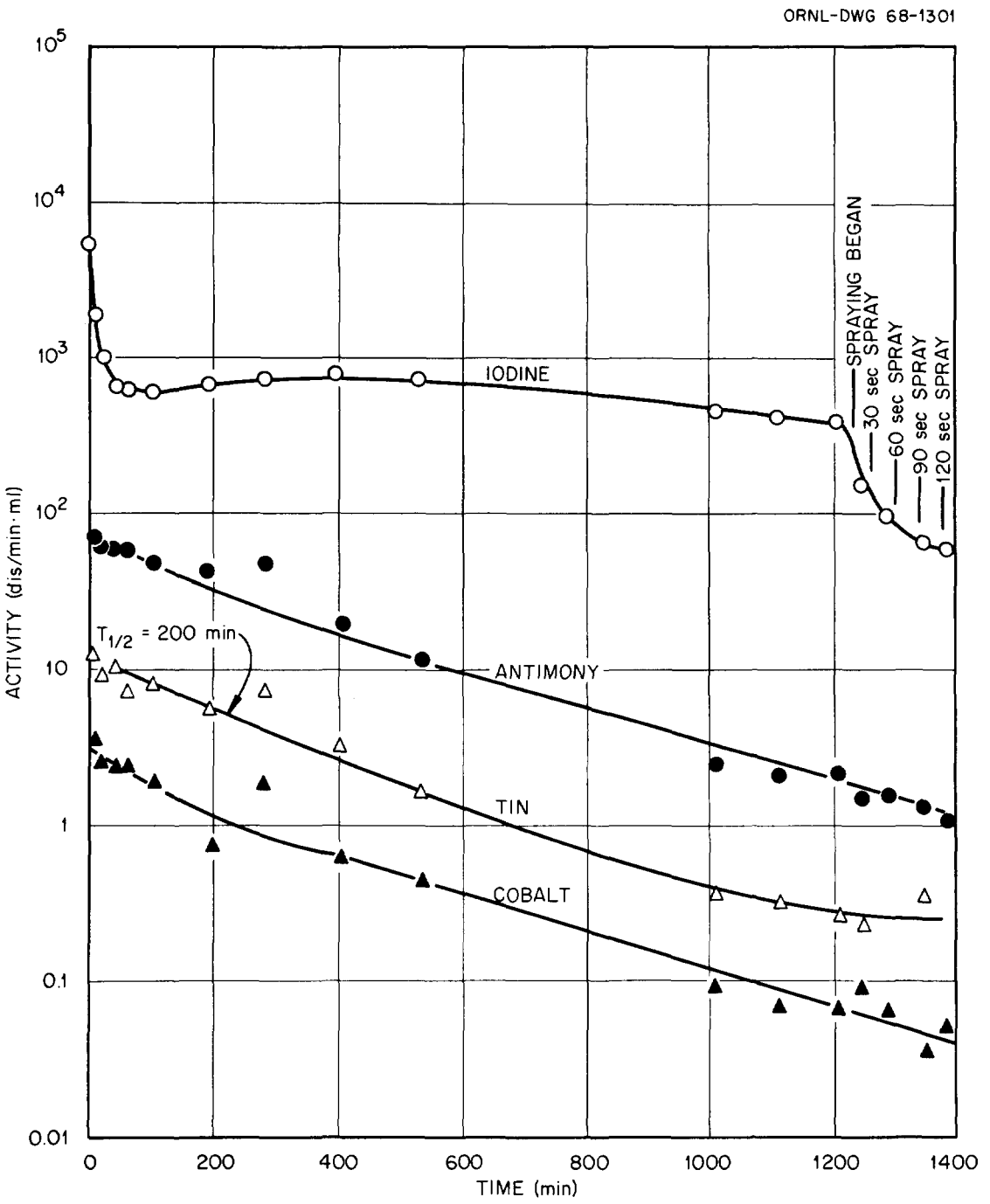

Results of Analyses of Sequential Gas Samples Taken During CRI Run 108 as Activity vs Time.

Fig. 18

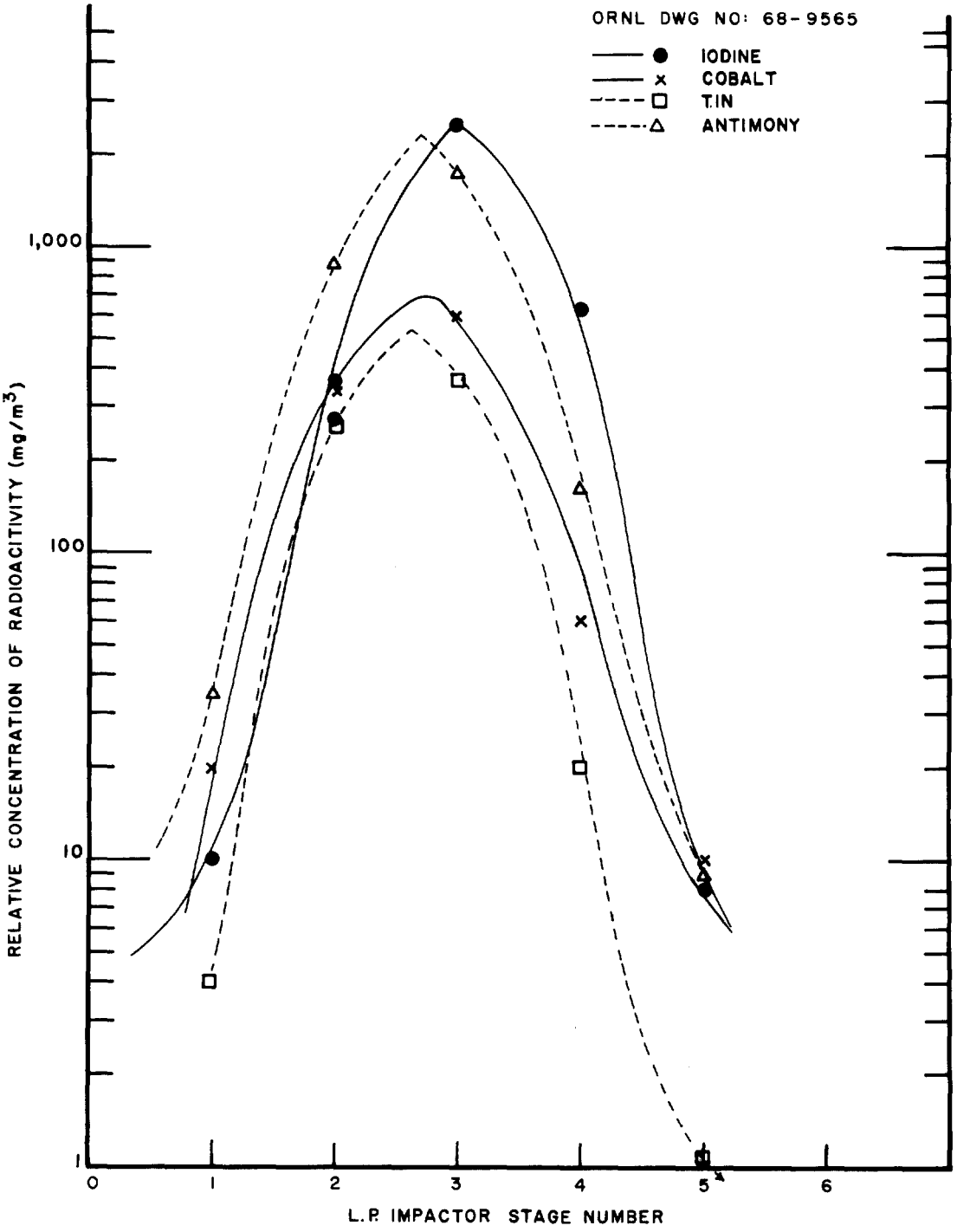

PARTICLE CLASSIFICATION OF RADIOIODINE ANTIMONY, TIN AND COBALT (RUN 108)

Fig. 19

Mark-II Impactor. In the first case (Run 112) a low concentration of U_3O_8 (2 mg/m^3) was observed and in the second case (Run 113) almost 1 gram/m^3 was provided.

As a test of the agglomeration processes a total particle number count was made during the same time that the particle concentration and size analyses were made. These results are shown in Fig. 20. That smaller particle sizes were observed in the lower concentration U_3O_8 aerosol is shown in Fig. 21. In the dilute aerosol, the change in mass median diameter decreased from 0.13 microns to about 0.05 microns after 30 hr. In the higher concentration aerosol, the decrease was from 0.40 to 0.17 μ in the same time.

3.9 Analysis of the CRI Aerosols by the Effect of Stirred Settling

In both the SnO_2 and U_3O_8 aerosols an analysis of the settling behavior was applied to the gas phase concentration data. Particle sizes (Stokes, d_8) calculated from the rate of aerosol settling are in fair agreement with particle sizes measured by the low pressure cascade impactor in this study.

The correlation for stirred settling given in "Handbook on Aerosols" by Sinclair[18] and in Green and Lane Chapter 6 was used:

$$-\frac{d}{dt} \log M_t = 1.3 \times 10^5 \frac{\rho}{h} d_8^2 \quad . \tag{13}$$

The comparisons are given in Tables 3 and 4. Note that d_8 is the diameter calculated from stirred settling rates; d_6 (the mass median diameter) and d_g (the count median diameter) were then calculated from d_8 by assuming values of σ and using the equation

$$\log d_m = \log d_g + 2.303 \frac{m}{2} \log^2 \sigma \quad .$$

The difference between d_8, d_6, and d_g depends upon σ and the equations are accurate only for spherical particles which have a log-normal size distribution. The tables also show the values of mass median diameter (d_g) and σ as measured by the low-pressure cascade impactor.

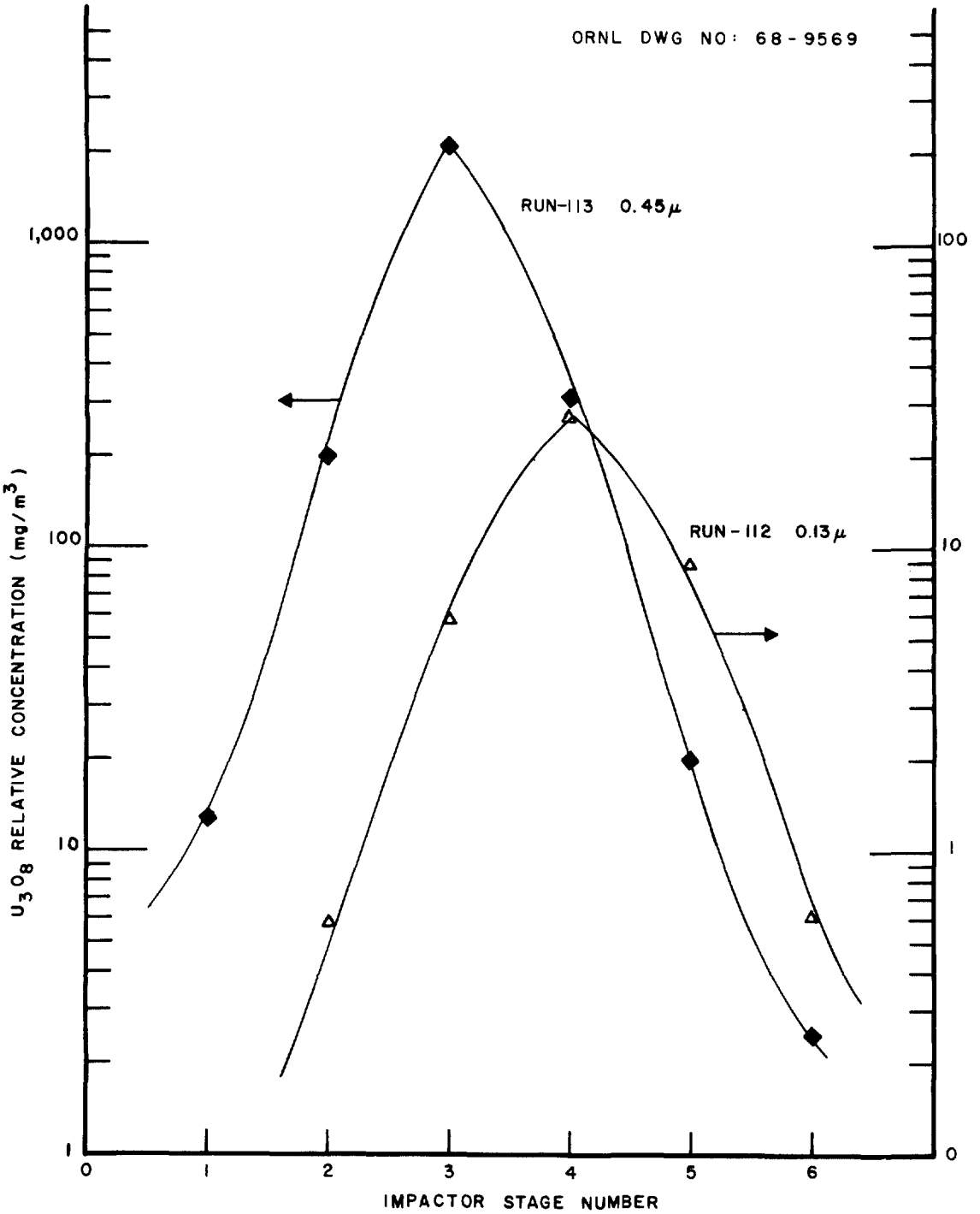

CLASSIFICATION OF URANIUM OXIDE PARTICLES
AT TWO CONCENTRATION LEVELS

Fig. 20

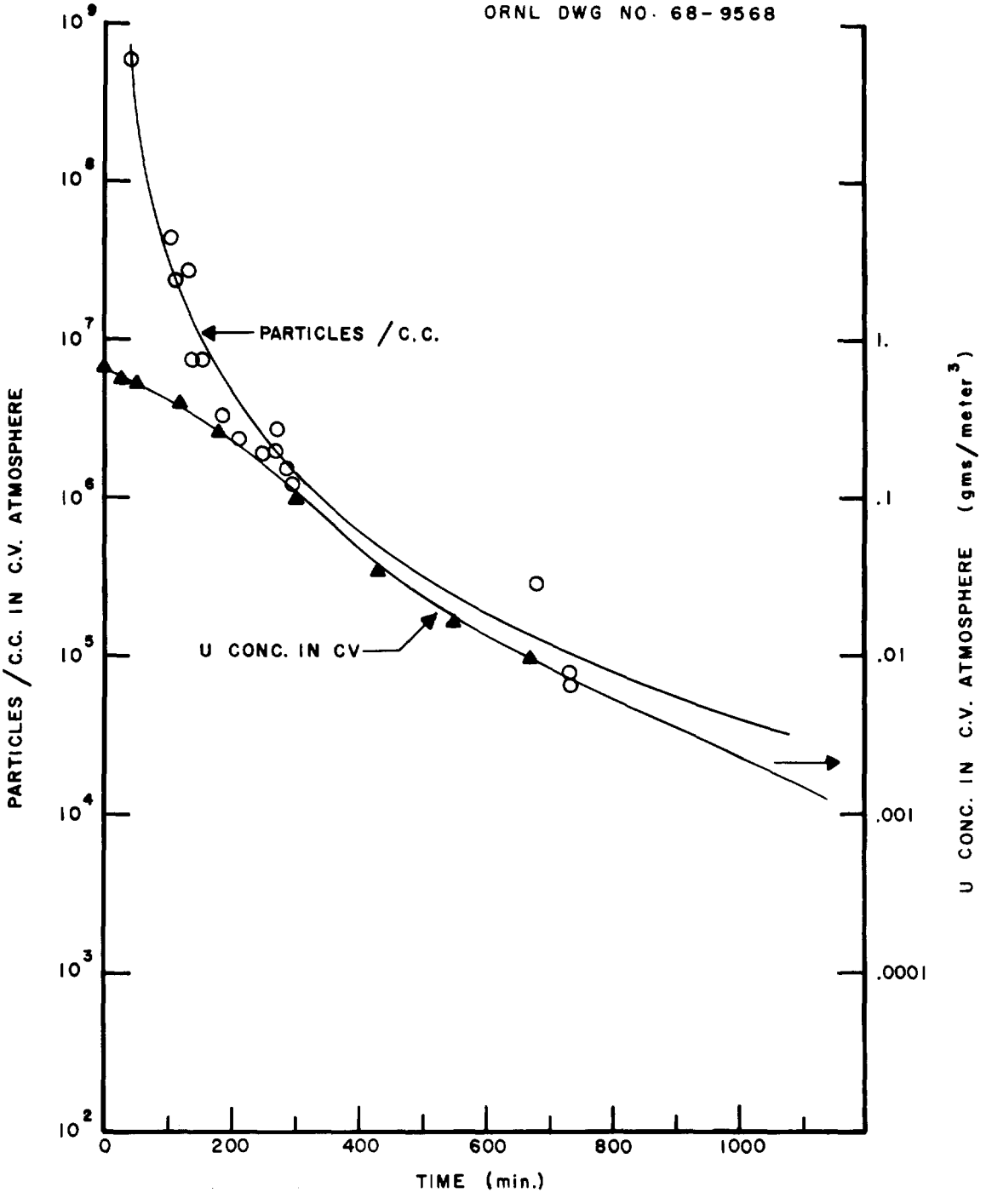

CHANGE IN AEROSOL CONCENTRATION IN RUN 113

Fig. 21

Table 3. A Comparison of the Size of Tin Oxide Particles Calculated from Settling Velocity with the Impactor Analysis Size

CRI 108 (SnO_2)

Test No.	Calculated Particle Diameter (μ)* (Settling) d_8	(Mass Med.) d_6	(Geometric) d_g	Measured Dia. L. P. Impactor Mass Med. d_6
CRI 107 (Initial slope)	0.86	0.61	0.216	0.31 (σ = 1.8)
CRI 108 (Constant slope)	0.75	0.53	0.188	0.55 (σ = 1.7)

*σ assumed = 1.8

Table 4. A Comparison of the Size of Uranium Oxide Particles Calculated by Settling Velocity with the Impactor Analysis Size CRI 113 (U_3O_8)

Time Interval	Half Time	Settling Velocity V	Calculated Particle Diameter (μ) (Mean d_8)	(Mass Med. if σ = 2.0)	(Mass Med. if σ = 2.5)	Measured* Values d_6	σ
Min.	Min.	cm/sec					
0-120	140	1.65×10^{-2}	0.74	0.46	0.32	0.40	1.8
180-430	85	2.72×10^{-2}	0.96	0.60	0.42	0.30	2.3
1200-1550	200	1.15×10^{-2}	0.61	0.38	0.265	0.20	2.2

*From impactor analysis.

By sampling frequently with the Mark-II Impactor, a gradual change in the aerosol characteristics including the standard deviation is noted. Figure 22 shows the results of two analyses over the time interval of most importance for the two uranium oxide test aerosols.

A similarly useful analysis has been proposed by Davis[19] based on the concept that agglomeration and other natural processes tend to preserve the natural size distribution of the particles. In noting the change in mean mass diameter over the essential life span of the aerosol (reduction of 10^3) the "self-preserving" size rule proposed by Davis is not seriously in conflict with our observations. The size appears to remain nearly constant for a period needed to reduce the concentration by about 100 before the smaller sizes and lower settling rates are noted (Fig. 23).

4. DISCUSSION

From the initial studies of particle behavior in simulated reactor containment vessels with the help of a new size classification device, it appears that given maximum particle size, by independent measurement, the removal rate can be calculated from the theory of stirred settling. It also appears that over the time range of major interest the assumption of "self-preserving" size distribution is reasonably in agreement with the observations. On the other hand, agglomeration theory does not seem to be compatible with the observed stability of the aerosol. It is therefore concluded that a purely theoretical treatment probably does not adequately describe all the results of this study.

ORNL DWG NO: 68-9567

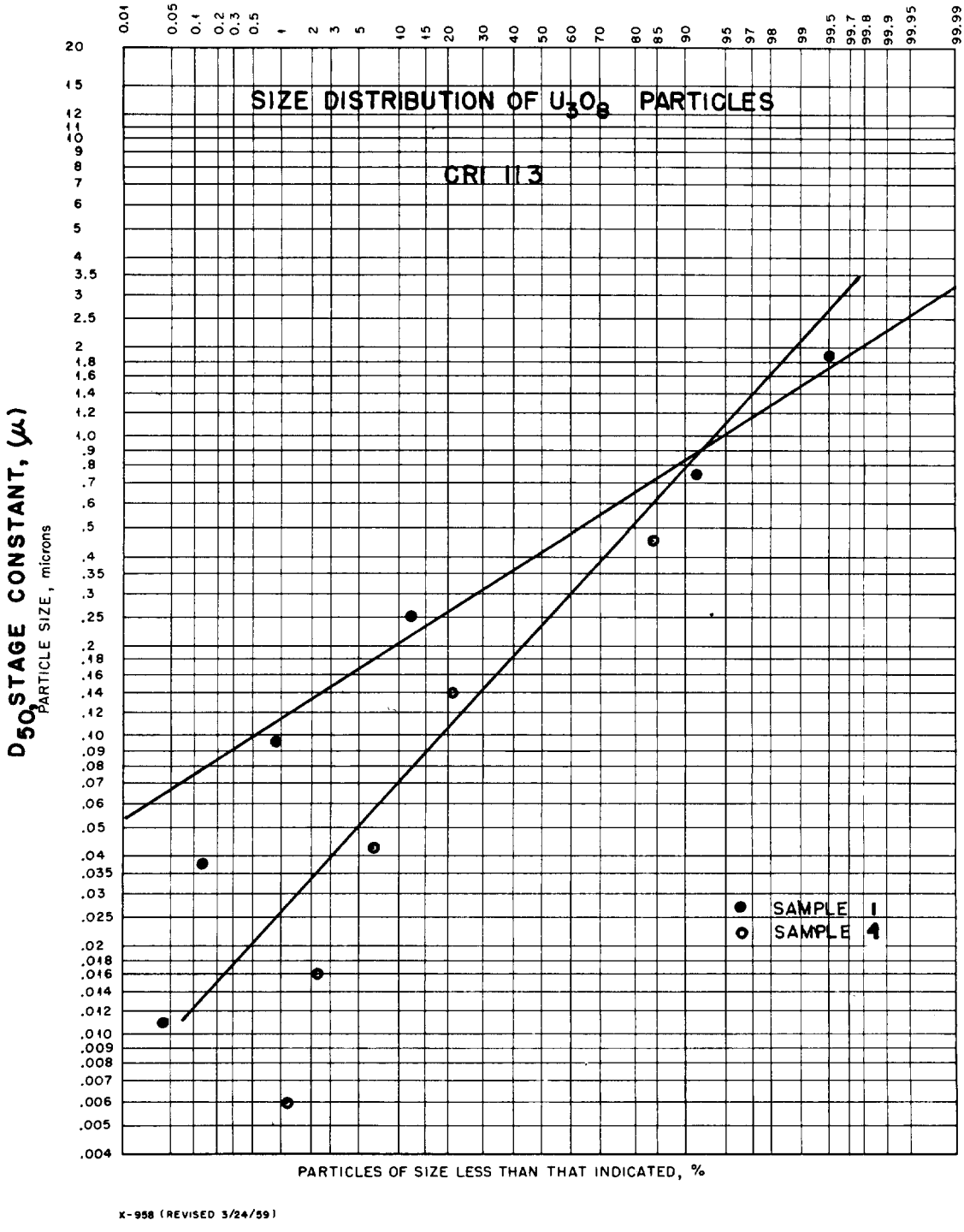

Fig. 22

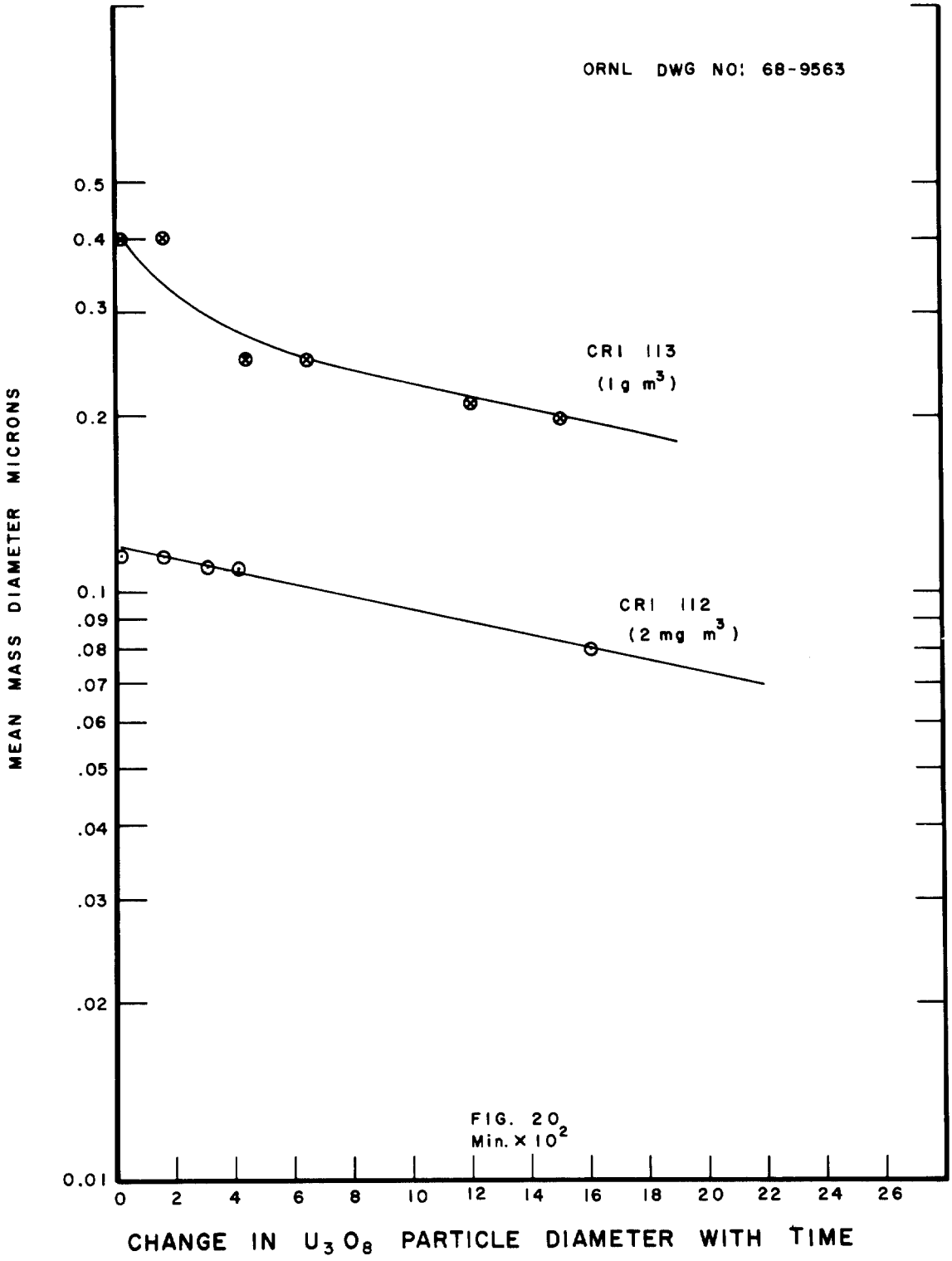
ORNL DWG NO: 68-9563
MEAN MASS DIAMETER MICRONS
0.5
0.4
0.3
0.2
0.1
.09
.08
.07
.06
.05
.04
.03
.02
0.01
CRI 113
(1 g m3)
CRI 112
(2 mg m3)
FIG. 20
Min. X 10^2
0
2
4
6
8
10
12
14
16
18
20
22
24
26
CHANGE IN U3O8 PARTICLE DIAMETER WITH TIME

Fig. 23

5. SUMMARY

Submicron particles are an important subject of investigation in nuclear safety research. Instruments which would separate these particles into different size fractions, and make each size fraction available for further analysis are of great interest. Cascade impactors are ordinarily limited to particle sizes greater than 0.5 μ and are therefore not adequate for this task. But this range can be extended to very small sizes by operating the impactor at low pressure. This makes the cascade impactor of genuine use in nuclear safety research. Small particles which would not impact under normal pressure are deposited on the impaction plates, at reduced pressure, by a slip effect in the gas stream. The range of application is thus extended to particles of less than 0.01 μ diameter.

The Mark-II sampler is recommended for use in Nuclear Safety containment research. It separates particles in the size range from 0.01 μ to several microns. It is easily assembled or disassembled — for instance, in a hot cell. (Disassembly and reassembly for another sample can be accomplished on cold material in a few minutes.) It is designed with throw-away plates which facilitate decontamination and measurement by radioactivity.

6. ACKNOWLEDGMENT

We wish to acknowledge the Particle Technology Laboratory at the University of Minnesota for the use of their aerosol generators. In particular, the aid and hospitality of B.Y.H. Liu and A. R. McFarland are acknowledged.

We wish also to express appreciation for the help of G. E. Creek for supplying a computer code for some of the calculations and of R. J. Davis and R. A. Lorenz for proof reading the manuscript and adding helpful interpretations.

7. REFERENCES

1. C. J. Barton, "The Hazard of Dispersed Plutonium Particles," Nuclear Safety 7, 468 (1966).

2. G. W. Parker, G. E. Creek and W. J. Martin, Fission Product Release from UO_2 by High Temperature Diffusion and Melting in Helium and Air, ORNL-CF-60-12-14 (1960), see also ORNL-NSIC-5.

3. G. W. Parker and H. Buchholz, Nuclear Safety Program Annual Progress Report for Period Ending December 31, 1966, USAEC Report ORNL-4071, p. 196, Oak Ridge National Laboratory.

4. G. W. Parker and H. Buchholz, "Low Pressure Cascade Impactor as a Tool for the Study of Size Distribution of Fission Product Aerosols," Trans. Am. Nuclear Society 10(1), 338 (1967).

5. K. R. May, "The Cascade Impactor, An Instrument for Sampling Coarse Aerosols," J. Sci. Instr. 22, 187 (1945).

6. W. E. Ranz, J. B. Wong, "Impaction of Dust and Smoke Particles on Surface and Body Collectors," Ind. Eng. Chem. 44, 1371 (1952).

7. C. N. Davies, M. Aylward, "The Trajectories of Heavy Solid Particles in a Two Dimensional Jet of Ideal Fluid Impinging Normally Upon a Plate," Proc. Phys. Soc. London 64, 889 (1951).

8. A. R. McFarland, H. W. Zeller, Study of a Large Volume Impactor for High-Altitude Aerosol Collection, TID-18624 (1963).

9. H. Schlichting, Boundary Layer Theory, McGraw-Hill, New York, Chapter 1 (1955).

10. S. C. Stern et al., "Collection Efficiency of Jet Impactors at Reduced Pressure," Ind. Eng. Chem. Fundamentals 1, 273 (1962).

11. R. A. Millikan, "The General Law of Fall of a Small Spherical Body Through Gas and Jets Bearing Upon the Nature of Molecular Reflection from Surfaces," Phys. Rev. 22, 1 (1923).

12. T. T. Mercer, The Stage Constants of Cascade Impactors, LF-12 (1963).

13. G. W. Parker and H. Buchholz, Nuclear Safety Program Annual Progress Report for Period Ending December 31, 1966, USAEC Report ORNL-4071, pp. 52 and 193, Oak Ridge National Laboratory.

14. G. W. Parker and H. Buchholz, Size Classification of Submicron Particles by a Low Pressure Cascade Impactor, USAEC Report ORNL-4226, June 1968.

15. K. T. Whitby et al., "Homogeneous Aerosol Generators," Int. J. Air Wat. Poll. Vol. 9, 263 (1965).

16. Andersen Samplers a Consulting Service, 1074 Ash Ave., Provo, Utah, U.S.A.

17. J. C. Couchman, Use of Cascade Impactors for Analyzing Airborne Particles of High Specific Gravity, CONF-650407 (1965), p. 1162.

18. H. F. Johnstone, Ed., "AEC Handbook on Aerosols," STR-10-1, pp. 64-76 (1963).

19. R. J. Davis, R. E. Adams, et al., Nuclear Safety Program Annual Progress Report for Period Ending December 31, 1967 USAEC Report ORNL-4228, p. 148, Oak Ridge National Laboratory.

GIESEKE: You mentioned the Andersen impactor as an example. Is that what you used in the study?

PARKER: This is a variation of the Andersen, yes.

GIESEKE: My experience has been that the Andersen impactor does not give a very sharp cut off with respect to particle size. However, it does have one good point in that it has relatively low wall losses operating under normal atmospheric conditions.

Did you check the wall losses during operation at reduced pressures? I suspect that they would go way up.

PARKER: We examined wall loss and if you look at Report ORNL-4226, the evidence is that it is indeed quite low, e.g. in the one to two per cent region.

GIESEKE: Even under the reduced pressure?

PARKER: Even under reduced pressure. There's one other factor which gets into particle analysis by this method and that is fracturing. Now, we have evidence also in the paper which says this is not a significant problem.

CORDES: Dr. Parker, we have had some trouble with the Andersen with regard to the stage constants. The stage constants do not seem to stay constant but depend on a constant concentration. That is, when you first start operating the sampler, right underneath each little hole, you build a little mound of particulates that changes the aerosol dynamics which changes the stage constants. Did you take this into account?

PARKER: You must not do that (overload the Impactor).

FIRST: The next paper is entitled, "Off-Gas Systems for Nuclear Contaminated Combustibles." I must apologize for an error in the program which neglected to give the author's name. It is Rex Gaskins of the Dow Chemical Company, Rocky Flats Division.